DO-TH 12/16
EOS-2012-02
SI-HEP-2012-21
QFET-2012-02

General Analysis of $\bar{B} \to \bar{K}^{(*)}\ell^+\ell^-$ Decays at Low Recoil

Christoph Bobeth
Excellence Cluster Universe, Technische Universität München, D-85748 Garching, Germany

Gudrun Hiller
Institut für Physik, Technische Universität Dortmund, D-44221 Dortmund, Germany

Danny van Dyk
Institut für Physik, Technische Universität Dortmund, D-44221 Dortmund, Germany and
Theoretische Physik 1, Naturwissenschaftlich-Technische Fakultät,
Universität Siegen, Walter-Flex-Straße 3, D-57068 Siegen, Germany

We analyze the angular distributions of $\bar{B} \to \bar{K}^*(\to \bar{K}\pi)\ell^+\ell^-$ and $\bar{B} \to \bar{K}\ell^+\ell^-$ decays in the region of low hadronic recoil in a model-independent way by taking into account the complete set of dimension-six operators $[\bar{s}\Gamma b][\bar{\ell}\Gamma'\ell]$. We obtain several novel low-recoil observables with high sensitivity to non-standard-model Dirac structures, including CP-asymmetries which do not require flavor tagging. The transversity observables $H_T^{(1,3,4,5)}$ are found to be insensitive to hadronic matrix elements and their uncertainties even when considering the complete set of operators. In the most general scenario we show that the low recoil operator product expansion can be probed at the few-percent level using the angular observable J_7. Higher sensitivities are possible assuming no tensor contributions, specifically by testing the low-recoil relation $|H_T^{(1)}| = 1$. We explicitly demonstrate the gain in reach of the low-recoil observables in accessing the ratio $|\mathcal{C}_9/\mathcal{C}_{10}|$ compared to the forward-backward asymmetry, and probing CP-violating right-handed currents $\mathrm{Im}\,\mathcal{C}_{10'}$. We give updated Standard Model predictions for key observables in $\bar{B} \to \bar{K}^{(*)}\ell^+\ell^-$ decays.

I. INTRODUCTION

Flavor Changing Neutral Current (FCNC) decays of beauty hadrons have a high sensitivity to New Physics (NP) since the corresponding Standard Model (SM) contributions are loop and flavor suppressed. In addition, the large value of the b-quark mass facilitates the control of power corrections.

The large number of complementary observables and the excellent accessibility at contemporary high energy experiments, in particular for muons, highlights the exclusive FCNC decays $\bar{B} \to \bar{K}^*(\to \bar{K}\pi)\ell^+\ell^-$. In the kinematic region of low hadronic recoil, where the emitted K^* is soft in the B-rest frame, a local Operator Product Expansion (OPE) can be performed [1, 2]. Together with the improved Isgur-Wise relations [1, 3, 4], this results in a simple structure of the transversity decay amplitudes at leading order in $1/m_b$ [4]

$$A_i^{L,R} \propto C^{L,R} f_i, \qquad i = \perp, \parallel, 0\,, \tag{1}$$

factorizing into universal short-distance coefficients $C^{L,R}$ and form factors f_i. This feature allows to extract short-distance couplings without long-distance pollution, and vice versa, as well as to test the performance of the OPE [4, 5].

The opposite kinematical region of large recoil has been subjected to the question of optimized observables as well, *e.g.,* [6–13]. Several proposals exploit specifically that QCD factorization (QCDF) [14, 15] at leading order maintains universal short-distance coefficients for $A_\perp^{L,R}$ and $A_\parallel^{L,R}$, while Eq. (1) is broken for $i = 0$ at lowest order, and for all $i = \perp, \parallel, 0$ at order $1/m_b$.

The additional benefit of the low recoil region is the strong parametric suppression of the subleading $1/m_b$ corrections to the decay amplitudes at the order of a few percent [1, 4]. Together with an angular analysis [16] this enables a rich flavor physics program, complementing the large recoil region. One application is to extract form factor ratios f_i/f_j from data, as has recently been demonstrated in [17, 18].

The key questions addressed in this work are:

i) To which extent is Eq. (1) and its benefits preserved in the presence of operators beyond the SM ones?

ii) What are the optimal low recoil observables model-independently?

iii) What is their sensitivity to NP?

iv) What is the sensitivity to potential corrections to the OPE?

To answer the above questions we perform a most general, model-independent analysis of the decays $\bar{B} \to \bar{K}^*(\to \bar{K}\pi)\ell^+\ell^-$ and $\bar{B} \to \bar{K}\ell^+\ell^-$. In terms of semileptonic dimension-six operators $[\bar{s}\,\Gamma\,b]\,[\bar{\ell}\,\Gamma'\,\ell]$ this concerns the chirality-flipped partners of the SM ones, (pseudo-)scalar and tensor operators. We compute various decay distributions and asymmetries.

The plan of the paper is as follows: The effective theory including the operator basis is given in Section II.

We present low recoil observables and relations from different operator sets in Section III and Section IV for $\bar{B} \to \bar{K}^*(\to \bar{K}\pi)\ell^+\ell^-$ and $\bar{B} \to \bar{K}\ell^+\ell^-$, respectively. In Section V we study the sensitivity of the low recoil observables to even small NP effects. The sensitivity to OPE corrections is worked out in Section VI as well as a brief discussion of S-wave backgrounds. We conclude in Section VII.

In several appendices we give formulae and subsidiary information. In Appendix A we discuss the full angular decay distribution in $\bar{B} \to \bar{K}^*(\to \bar{K}\pi)\ell^+\ell^-$ decays. In Appendix B we present the angular observables in terms of the transversity amplitudes for the complete set of semileptonic $|\Delta B| = |\Delta S| = 1$ operators. In Appendix C we detail the transversity amplitudes that parametrize the tensor contribution to the matrix element. An update of the SM predictions for the key observables in $\bar{B} \to \bar{K}^*\ell^+\ell^-$ and $\bar{B} \to \bar{K}\ell^+\ell^-$ decays is given in Appendix D.

II. THE EFFECTIVE HAMILTONIAN

Rare semileptonic $|\Delta B| = |\Delta S| = 1$ decays are described by an effective Hamiltonian

$$\mathcal{H}_{\text{eff}} = -\frac{4\,G_F}{\sqrt{2}} V_{tb} V_{ts}^* \frac{\alpha_e}{4\pi} \sum_i \mathcal{C}_i(\mu) \mathcal{O}_i(\mu). \tag{2}$$

Here, G_F denotes Fermi's constant, α_e the fine structure constant and unitarity of the Cabibbo-Kobayashi-Maskawa (CKM) matrix V has been used. The subleading contribution proportional to $V_{ub}V_{us}^*$ has been neglected.

The renormalization scale μ, which appears in the short-distance couplings $\mathcal{C}_i$ and the matrix elements of the operators $\mathcal{O}_i$, is of the order of the b-quark mass. In the following we suppress the dependence of the Wilson coefficients $\mathcal{C}_i$ on the scale μ.

In the SM $b \to s\,\ell^+\ell^-$ processes are mainly governed by the operators $\mathcal{O}_{7,9,10}$ which will be referred to as the SM operator basis. Beyond the SM chirality-flipped ones $\mathcal{O}_{7',9',10'}$, collectively denoted here by SM', may appear. The SM and SM' operators are written as [6, 8, 19]

$$\begin{aligned} \mathcal{O}_{7(7')} &= \frac{m_b}{e} \big[\bar{s}\sigma^{\mu\nu} P_{R(L)} b\big]\, F_{\mu\nu}\,, \\ \mathcal{O}_{9(9')} &= \big[\bar{s}\gamma_\mu P_{L(R)} b\big]\big[\bar{\ell}\gamma^\mu \ell\big]\,, \\ \mathcal{O}_{10(10')} &= \big[\bar{s}\gamma_\mu P_{L(R)} b\big]\big[\bar{\ell}\gamma^\mu\gamma_5 \ell\big]\,. \end{aligned} \tag{3}$$

Furthermore, we allow for scalar and pseudo-scalar operators, referred to as S and P,

$$\begin{aligned} \mathcal{O}_{S(S')} &= \big[\bar{s} P_{R(L)} b\big]\big[\bar{\ell}\ell\big]\,, \\ \mathcal{O}_{P(P')} &= \big[\bar{s} P_{R(L)} b\big]\big[\bar{\ell}\gamma_5 \ell\big]\,, \end{aligned} \tag{4}$$

which includes the chirality-flipped ones, as well as tensor operators, referred to as T and T5,

$$\begin{aligned} \mathcal{O}_T &= [\bar{s}\sigma_{\mu\nu} b]\big[\bar{\ell}\sigma^{\mu\nu}\ell\big]\,, \\ \mathcal{O}_{T5} &= [\bar{s}\sigma_{\mu\nu} b]\,\big[\bar{\ell}\sigma^{\mu\nu}\gamma_5 \ell\big]\,. \end{aligned} \tag{5}$$

Note that $\mathcal{O}_{T5} = -i/2\,\varepsilon^{\mu\nu\alpha\beta}\,[\bar{s}\sigma_{\mu\nu} b]\big[\bar{\ell}\sigma_{\alpha\beta}\ell\big] = -\mathcal{O}_{TE}/2$, see Eq. (C16), as commonly used in the literature [19–21]. Current-current and QCD penguin operators $\mathcal{O}_{i\le 6}$, as well as the chromo-magnetic dipole operator $\mathcal{O}_8$ have to be included for a consistent description of $b \to s\ell^+\ell^-$ decays, for definition see [22]. The matrix elements of $\mathcal{O}_{1\ldots6,8}$ contribute to $b \to s + \{\gamma, g, \ell^+\ell^-\}$ processes via quark-loop effects. The latter are taken into account by means of the effective Wilson coefficients $\mathcal{C}_{7,8,9}^{\text{eff}}$. The effective Wilson coefficients are renormalization group invariant up to higher orders in the strong coupling constant α_s. In the case of exclusive decays the $1/m_b$ corrections in the large- and low-recoil region from QCDF [14, 15, 19] or SCET [23, 24] and the low-recoil OPE [1, 4, 5], respectively, should be included in the $\mathcal{C}_i^{\text{eff}}$. We evaluate α_e at $\mu = \mu_b = \mathcal{O}(m_b)$ which takes into account most of the NLO QED corrections [25, 26].

III. $\bar{B} \to \bar{K}^*\ell^+\ell^-$ AT LOW RECOIL

We study $\bar{B} \to \bar{K}^*(\to \bar{K}\pi)\ell^+\ell^-$ decays in the low recoil region for a generalized operator basis and detail the relevant observables and their relations. In Section III A we give the results using SM operators only. In Section III B, III C, III D we include either SM', S and P or T and T5 operators, respectively. Interference effects are worked out in Section III E.

The main results of this section are summarized in Table I, where the low recoil relations between the observables and the amount of their violations is given. Our results are based on the angular distribution presented in Appendix A, and the angular observables in Appendix B.

A. SM operators

The amplitude of the exclusive decays $\bar{B} \to \bar{K}^*\ell^+\ell^-$ can be treated at low recoil using an OPE and further matching onto HQET [1]. After application of the improved Isgur-Wise relations [1], one finds for the transversity amplitudes [4, 5], see also Eq. (1),

$$A_{0,\parallel}^{L,R} = -C^{L,R}\, f_{0,\parallel}\,, \qquad A_{\perp}^{L,R} = +C^{L,R}\, f_{\perp}\,. \tag{6}$$

The short-distance coefficients read

$$C^{L,R}(q^2) = \mathcal{C}_{79}^{\text{eff}}(q^2) \mp \mathcal{C}_{10}, \tag{7}$$

$$\mathcal{C}_{79}^{\text{eff}}(q^2) = \mathcal{C}_9 + \kappa \frac{2\,m_b M_B}{q^2} \mathcal{C}_7 + Y(q^2), \tag{8}$$

where Y denotes the matrix elements of the 4-quark operators, see [5] for details. Here, the matching correction $\kappa = 1 - 2\alpha_s/(3\pi)\ln\mu/m_b + \mathcal{O}(\alpha_s^2)$ arises from the lowest order improved Isgur-Wise relations. Its μ-dependence compensates the one of the dipole form factors $T_{1,2,3}$.

The term $\propto \mathcal{C}_7$ in Eq. (8) involves uncertainties from corrections at order $1/m_b$. However, since generically

$|\mathcal{C}_{9,10}| \gg |\mathcal{C}_7|$ (in the SM $\mathcal{C}_9 = 4.2$, $\mathcal{C}_{10} = -4.2$ and $\mathcal{C}_7 = -0.3$) the coefficient C^L can be regarded as strongly short-distance dominated whereas C^R yields only a numerically subleading contribution to observables. It follows that the subleading power corrections enter the amplitude at the few percent level.

The form factors f_i, also termed helicity form factors [27], can be written in terms of the usual heavy-to-light vector and axial-vector form factors V, $A_{1,2}$ as [4]

$$\begin{aligned}
\frac{f_\perp}{N} &= \frac{\sqrt{2\,\lambda}}{M_B + M_{K^*}} V\,, \\
\frac{f_\parallel}{N} &= \sqrt{2}\,(M_B + M_{K^*})\,A_1\,, \\
\frac{f_0}{N} &= \frac{(M_B^2 - M_{K^*}^2 - q^2)(M_B + M_{K^*})^2 A_1 - \lambda\, A_2}{2\,M_{K^*}(M_B + M_{K^*})\sqrt{q^2}}\,.
\end{aligned} \tag{9}$$

The normalization factor N depends on the invariant mass squared of the lepton pair, q^2, and is given in Eq. (B21). The kinematical factor $\lambda \equiv \lambda(M_B^2, M_{K^*}^2, q^2)$ is given in Eq. (C4).

The factorization into short-distance coefficients and form factors, Eq. (6), allows to identify suitable combinations of the observables J_i appearing in the angular distribution of $\bar{B} \to \bar{K}^*(\to \bar{K}\pi)\ell^+\ell^-$, see Appendix A for details. The angular observables depend on two short-distance parameters $\rho_{1,2}$ only,

$$\begin{aligned}
\frac{4}{3\beta_\ell^2}(2J_{2s} + J_3) &= 2\,\rho_1 f_\perp^2, \quad & -\frac{4}{3\beta_\ell^2} J_{2c} &= 2\,\rho_1 f_0^2\,, \\
\frac{4}{3\beta_\ell^2}(2J_{2s} - J_3) &= 2\,\rho_1 f_\parallel^2, & \frac{4\sqrt{2}}{3\beta_\ell^2} J_4 &= 2\,\rho_1 f_0 f_\parallel\,, \\
\frac{2\sqrt{2}}{3\beta_\ell} J_5 &= 4\,\rho_2 f_0 f_\perp, & \frac{2}{3\beta_\ell} J_{6s} &= 4\,\rho_2 f_\parallel f_\perp\,,
\end{aligned} \tag{10}$$

where

$$\rho_1 = \frac{1}{2}\left(|C^R|^2 + |C^L|^2\right) = \left|\mathcal{C}_{79}^{\rm eff}\right|^2 + \left|\mathcal{C}_{10}\right|^2, \tag{11}$$

$$\rho_2 = \frac{1}{4}\left(|C^R|^2 - |C^L|^2\right) = {\rm Re}\left(\mathcal{C}_{79}^{\rm eff}\,\mathcal{C}_{10}^*\right). \tag{12}$$

Note that $J_{7,8,9} = 0$ [4] and $J_{6c} = 0$ since neither S, P [8] nor T, T5 operators are present.

From Eq. (10) follow [4] the short- and long-distance free ratio

$$H_T^{(1)} \equiv \frac{\sqrt{2}J_4}{\sqrt{-J_{2c}\,(2J_{2s} - J_3)}}, \tag{13}$$

as well as the long-distance free ratios

$$H_T^{(2)} \equiv \frac{\beta_\ell J_5}{\sqrt{-2J_{2c}\,(2J_{2s} + J_3)}}, \tag{14}$$

$$H_T^{(3)} \equiv \frac{\beta_\ell J_{6s}}{2\sqrt{(2J_{2s})^2 - J_3^2}}. \tag{15}$$

Here we point out a further nontrivial observable, which does depend neither on form factors nor on short-distance physics:

$$H_T^{(1b)} \equiv -\frac{J_{2c}\,J_{6s}}{2\,J_4\,J_5}, \tag{16}$$

and which equals one. Note that this observable can be obtained via $H_T^{(1b)} = H_T^{(3)}/[H_T^{(1)} H_T^{(2)}]$. However, by using the definition Eq. (16) directly different J_i appear. This offers additional advantages in the experimental extraction from the angular distributions.

In addition, long-distance free CP asymmetries $a_{\rm CP}^{(1,2,3)}$ can be formed, which are related to the CP asymmetry of the decay rate, of the forward-backward asymmetry, and of $H_T^{(2,3)}$, respectively [5].

Furthermore, several short-distance free ratios of form factors (9) can be obtained

$$\begin{aligned}
\frac{f_0}{f_\parallel} &= \frac{\sqrt{2}J_5}{J_{6s}} = \frac{-J_{2c}}{\sqrt{2}J_4} \\
&= \frac{\sqrt{2}J_4}{2J_{2s} - J_3} = \sqrt{\frac{-J_{2c}}{2J_{2s} - J_3}}\,,
\end{aligned} \tag{17}$$

$$\frac{f_\perp}{f_\parallel} = \sqrt{\frac{2J_{2s} + J_3}{2J_{2s} - J_3}} = \frac{\sqrt{-J_{2c}\,(2J_{2s} + J_3)}}{\sqrt{2}J_4}\,, \tag{18}$$

$$\frac{f_0}{f_\perp} = \sqrt{\frac{-J_{2c}}{2J_{2s} + J_3}}\,. \tag{19}$$

They allow to extract information on form factors directly from the data [17, 18], providing a benchmark test for form factor determinations such as from lattice QCD.

To sum up, using SM-type operators only – which may or may not receive contributions from beyond the SM – the low recoil OPE predicts at leading order in $1/m_b$

$$\begin{aligned}
\frac{H_T^{(1)}}{{\rm sgn}(f_0)} &= H_T^{(1b)} = 1\,, & J_{7,8,9} &= 0\,, \\
H_T^{(2)} &= H_T^{(3)} = 2\,\frac{\rho_2}{\rho_1}\,,
\end{aligned} \tag{20}$$

and the observable form factor ratios given in Eqs. (17)-(19). As already stressed the subleading power corrections are parametrically suppressed and at the few percent level.

B. Chirality-flipped operators

Taking into account the chirality flipped operators the universal structure of the transversity amplitudes (6) is broken in part. One obtains in the (SM+SM') model

$$A_{0,\parallel}^{L,R} = -C_-^{L,R}\, f_{0,\parallel}, \qquad A_\perp^{L,R} = +C_+^{L,R}\, f_\perp, \tag{21}$$

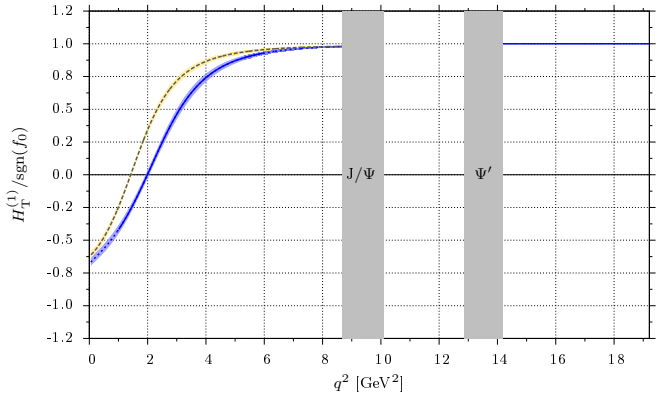

(a)

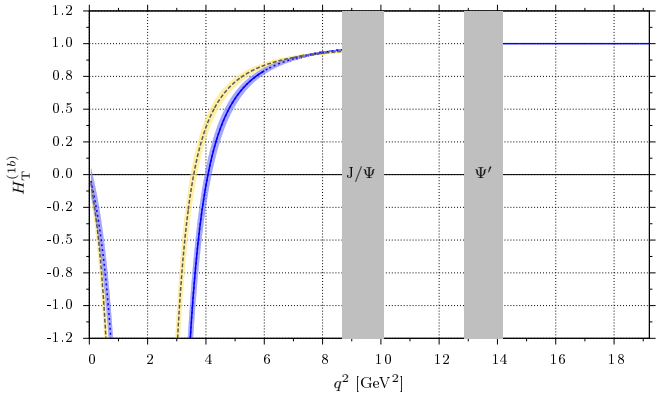

(b)

FIG. 1: $H_T^{(1)}/\mathrm{sgn}(f_0)$ (a) and $H_T^{(1b)}$ (b) in the large and low recoil regions, below and above the experimentally vetoed narrow charmonium backgrounds (vertical grey bands) from $\bar{B} \to J/\Psi(\to \ell^+\ell^-)\bar{K}^*$ and $\bar{B} \to \Psi'(\to \ell^+\ell^-)\bar{K}^*$, respectively. Shown are the SM prediction (blue solid) and the (SM+SM') benchmark point (black dashed) with their respective uncertainty bands (darker (blue) and lighter (gold)), respectively. See text for details.

where

$$C_-^{L,R}(q^2) = \mathcal{C}_{79}^{\rm eff} - \mathcal{C}_{7'9'}^{\rm eff} \mp (\mathcal{C}_{10} - \mathcal{C}_{10'}), \tag{22}$$

$$C_+^{L,R}(q^2) = \mathcal{C}_{79}^{\rm eff} + \mathcal{C}_{7'9'}^{\rm eff} \mp (\mathcal{C}_{10} + \mathcal{C}_{10'}), \tag{23}$$

$$\mathcal{C}_{7'9'}^{\rm eff}(q^2) = \mathcal{C}_{9'} + \kappa \frac{2\, m_b M_B}{q^2} \mathcal{C}_{7'} + Y'(q^2). \tag{24}$$

Here $\mathcal{C}_{7'9'}^{\rm eff}$ is defined analogously to $\mathcal{C}_{79}^{\rm eff}$, *i.e.*, Y' denotes the matrix element of the chirality-flipped 4-quark operators.

The angular observables J_i in (SM+SM') read

$$\begin{aligned} \frac{4}{3\beta_\ell^2}(2J_{2s}+J_3) &= 2\,\rho_1^+ f_\perp^2, & -\frac{4}{3\beta_\ell^2}J_{2c} &= 2\,\rho_1^- f_0^2, \\ \frac{4}{3\beta_\ell^2}(2J_{2s}-J_3) &= 2\,\rho_1^- f_\parallel^2, & \frac{4\sqrt{2}}{3\beta_\ell^2}J_4 &= 2\,\rho_1^- f_0 f_\parallel, \\ \frac{2\sqrt{2}}{3\beta_\ell}J_5 &= 4\,\mathrm{Re}(\rho_2) f_0 f_\perp, & \frac{2}{3\beta_\ell}J_{6s} &= 4\,\mathrm{Re}(\rho_2) f_\parallel f_\perp, \end{aligned} \tag{25}$$

$$\frac{4\sqrt{2}}{3\beta_\ell^2}J_8 = 4\,\mathrm{Im}(\rho_2) f_0 f_\perp, \qquad -\frac{4}{3\beta_\ell^2}J_9 = 4\,\mathrm{Im}(\rho_2) f_\parallel f_\perp,$$

where $J_7 = 0$ still holds and ρ_1 and ρ_2 have been generalized to

$$\begin{aligned} \rho_1^\pm &\equiv \frac{1}{2}\left(|C_\pm^R|^2 + |C_\pm^L|^2\right), \\ \rho_2 &\equiv \frac{1}{4}\left(C_+^R C_-^{R*} - C_-^L C_+^{L*}\right). \end{aligned} \tag{26}$$

Switching off the chirality flipped operators one recovers $C_+^L = C_-^L = C^L$ (and analogously for $L \to R$), such that $\rho_1^+ = \rho_1^- = \rho_1$.

In (SM+SM'), the asymmetries $H_T^{(2,3)}$, defined in Eqs. (14)-(15), read

$$H_T^{(2)} = 2\,\frac{\mathrm{Re}(\rho_2)}{\sqrt{\rho_1^- \cdot \rho_1^+}}, \qquad H_T^{(3)} = 2\,\frac{\mathrm{Re}(\rho_2)}{\sqrt{\rho_1^- \cdot \rho_1^+}}. \tag{27}$$

They remain long-distance free. Furthermore, the low recoil predictions obtained in the SM basis

$$\frac{H_T^{(1)}}{\mathrm{sgn}(f_0)} = H_T^{(1b)} = 1, \quad H_T^{(2)} = H_T^{(3)}, \quad J_7 = 0 \tag{28}$$

remain intact.

In Fig. 1 we show $H_T^{(1)}$ and $H_T^{(1b)}$. While both equal one at low recoil in SM+SM', at large recoil both observables exhibit a nontrivial q^2-dependence and depend on short- and long-distance contributions. However, to lowest order form factors drop out in $H_T^{(1)}$ *cf.* [12] and $H_T^{(1b)}$. We show the residual uncertainty from the form factors and subleading $1/m_b$ corrections by the shaded bands. The SM is represented by the thin (blue) band, whereas the lighter shaded (gold) one corresponds to a scenario with $\mathcal{C}_{7',9'} = \mathcal{C}_{7,9}^{\rm SM}$, $\mathcal{C}_{10'} = -\mathcal{C}_{10}^{\rm SM}$, $\mathcal{C}_{7,9,10} = 0$. For numerical input, see Appendix D.

Since in (SM+SM') $J_{8,9} \neq 0$ two additional long-distance free ratios

$$H_T^{(4)} \equiv \frac{2J_8}{\sqrt{-2J_{2c}\,(2J_{2s}+J_3)}}, \tag{29}$$

$$H_T^{(5)} \equiv \frac{-J_9}{\sqrt{(2J_{2s})^2 - J_3^2}} \tag{30}$$

can be constructed. They obey

$$H_T^{(4)} = H_T^{(5)} = 2\,\frac{\mathrm{Im}(\rho_2)}{\sqrt{\rho_1^- \cdot \rho_1^+}}. \tag{31}$$

We point out a further nontrivial observable, which depends neither on form factors nor on short-distance physics:

$$H_T^{(1c)} \equiv 2\,\frac{J_4\, J_8}{J_{2c}\, J_9}, \tag{32}$$

where in (SM+SM')

$$H_T^{(1c)} = 1\,. \tag{33}$$

For $H_T^{(1c)}$ an analogous comment as on $H_T^{(1b)}$ applies, see text below Eq. (16).

The transverse asymmetries $H_T^{(2,3,4,5)}$ are driven by the real and imaginary part of ρ_2, written as

$$\mathrm{Re}(\rho_2) = \mathrm{Re}(\mathcal{C}_{79}^{\mathrm{eff}}\,\mathcal{C}_{10}^{*} - \mathcal{C}_{7'9'}^{\mathrm{eff}}\,\mathcal{C}_{10'}^{*})\,, \tag{34}$$

$$\mathrm{Im}(\rho_2) = \mathrm{Im}(\mathcal{C}_{7'9'}^{\mathrm{eff}}\,\mathcal{C}_{79}^{\mathrm{eff}*} - \mathcal{C}_{10}\,\mathcal{C}_{10'}^{*})\,, \tag{35}$$

where $\mathrm{Im}(\rho_2)$ vanishes for $\mathcal{C}_{i'} = 0$ including vanishing chirality-flipped four-quark operators. Real-valued SM+SM' Wilson coefficients can still induce somewhat suppressed, finite values of $H_T^{(4,5)}$ through the absorptive contributions in the matrix elements of the four-quark operators Y and Y', by $\mathrm{Im}(\rho_2) = \mathrm{Re}\,\mathcal{C}_{79}^{\mathrm{eff}}\,\mathrm{Im}\,Y' - \mathrm{Re}\,\mathcal{C}_{7'9'}^{\mathrm{eff}}\,\mathrm{Im}\,Y$. Note that in the SM in the low recoil region $\mathrm{Im}\,Y_{\mathrm{SM}} \sim 0.2 - 0.3$ [5]. In any case, $H_T^{(4,5)}$ are null tests of the SM. A SM background to right-handed currents arises at higher order in the OPE including and counting m_s/m_b-terms as such and enters $H_T^{(4,5)}$ with additional parametric suppression by α_s or $\mathcal{C}_7/\mathcal{C}_9$ [1, 2].

Combinations result in further useful observables which do not depend on form factors either:

$$\frac{H_T^{(4)}}{H_T^{(2)}} = \frac{2}{\beta_\ell}\frac{J_8}{J_5}\,, \qquad \frac{H_T^{(5)}}{H_T^{(3)}} = -\frac{2}{\beta_\ell}\frac{J_9}{J_{6s}}\,. \tag{36}$$

Both equal $\mathrm{Im}(\rho_2)/\mathrm{Re}(\rho_2)$ in (SM+SM').

Since $J_{8,9}$ are naive T-odd these angular observables give optimal access to CP violation in the presence of small strong phases [7]. Since both $J_{8,9}$ are also CP-odd, $H_T^{(4,5)}$ can be measured from B-meson samples without tagging and give rise to a further long-distance-free CP asymmetry defined as

$$a_{\mathrm{CP}}^{(4)} = \begin{cases} \dfrac{\sqrt{2}(J_8 - \bar{J}_8)}{\sqrt{-(J_{2c}+\bar{J}_{2c})\left[2(J_{2s}+\bar{J}_{2s})+(J_3+\bar{J}_3)\right]}} \\ -\dfrac{J_9 - \bar{J}_9}{\sqrt{4\left(J_{2s}+\bar{J}_{2s}\right)^2 - \left(J_3+\bar{J}_3\right)^2}} \end{cases} \tag{37}$$

for $H_T^{(4)}$ and $H_T^{(5)}$, respectively. Here, the barred quantities are obtained by conjugating the weak phases. In terms of the short-distance coefficients $a_{\mathrm{CP}}^{(4)}$ reads

$$a_{\mathrm{CP}}^{(4)} = 2\,\frac{\mathrm{Im}(\rho_2 - \bar{\rho}_2)}{\sqrt{(\rho_1^+ + \bar{\rho}_1^+)\cdot(\rho_1^- + \bar{\rho}_1^-)}}\,. \tag{38}$$

The generalization of $a_{\mathrm{CP}}^{(3)}$ [5] is given by

$$a_{\mathrm{CP}}^{(3)} = 2\,\frac{\mathrm{Re}(\rho_2 - \bar{\rho}_2)}{\sqrt{(\rho_1^+ + \bar{\rho}_1^+)\cdot(\rho_1^- + \bar{\rho}_1^-)}}\,. \tag{39}$$

Due to the presence of ρ_1^+ and ρ_1^-, the generalization of the CP asymmetries $a_{\mathrm{CP}}^{(1)}$ and $a_{\mathrm{CP}}^{(2)}$ leads to a doubling

$$a_{\mathrm{CP}}^{(1,\pm)} \equiv \frac{\rho_1^\pm - \bar{\rho}_1^\pm}{\rho_1^\pm + \bar{\rho}_1^\pm}\,, \qquad a_{\mathrm{CP}}^{(2,\pm)} \equiv \frac{\dfrac{\rho_2}{\rho_1^\pm} - \dfrac{\bar{\rho}_2}{\bar{\rho}_1^\pm}}{\dfrac{\rho_2}{\rho_1^\pm} + \dfrac{\bar{\rho}_2}{\bar{\rho}_1^\pm}}\,. \tag{40}$$

In this case the CP asymmetry of the decay rate can not be related to any of the $a_{\mathrm{CP}}^{(1,\pm)}$ and is not long-distance free. However, from (25) it is straightforward to read off strategies to relate the $a_{\mathrm{CP}}^{(k,\pm)}$, $k = 1, 2$ to the J_i. In particular $a_{\mathrm{CP}}^{(1,-)}$ can be extracted from ratios involving J_{2c}, $(2J_{2s} - J_3)$, J_4, whereas $a_{\mathrm{CP}}^{(1,+)}$ requires $(2J_{2s} + J_3)$. In analogy to Eq. (2.37) of Ref. [5], the set b has to be restricted to $b = \{1, 3, 4\}$ for $a_{\mathrm{CP}}^{(2,-)}$ and to $b = 2$ for $a_{\mathrm{CP}}^{(2,+)}$.

In (SM+SM') short-distance free ratios of angular observables J_i exist for $f_0/f_\parallel$ as given in Eq. (17), and additionally

$$\frac{f_0}{f_\parallel} = \frac{\sqrt{2}J_8}{-J_9}\,. \tag{41}$$

Due to $(2J_{2s} + J_3) \propto \rho_1^+$, however, no short-distance free ratios can be formed which involve $f_\perp$. Hence, the observables F_L and $A_T^{(2,3)}$ are no longer short-distance free [4] either

$$F_L = \frac{\rho_1^- f_0^2}{\rho_1^-(f_0^2 + f_\parallel^2) + \rho_1^+ f_\perp^2}\,, \tag{42}$$

$$A_T^{(2)} = \frac{\rho_1^+ f_\perp^2 - \rho_1^- f_\parallel^2}{\rho_1^+ f_\perp^2 + \rho_1^- f_\parallel^2}\,, \qquad A_T^{(3)} = \sqrt{\frac{\rho_1^-}{\rho_1^+}}\,\frac{f_\parallel}{f_\perp}\,, \tag{43}$$

and the method used in [17] to extract form factor ratios would yield $\sqrt{\rho_1^-/\rho_1^+}(f_\parallel/f_\perp)$. With current data the correction factor is within $0.7 \le \sqrt{\rho_1^-/\rho_1^+} \le 1.4$ at 2 σ. Furthermore, we obtain the relation in (SM+SM')

$$A_T^{(3)} = \sqrt{\left(1 - A_T^{(2)}\right)\Big/\left(1 + A_T^{(2)}\right)}\,, \tag{44}$$

which can be checked experimentally.

C. Scalar and pseudo-scalar operators

The (S+P) operators modify the angular observables $J_{1c,5,6c,7}$ only. The respective NP contributions are driven by $A_0\Delta_{S,P}$, where A_0 denotes the $B \to K^*$ axial-vector form factor and $\Delta_{S,P} \equiv \mathcal{C}_{S,P} - \mathcal{C}_{S',P'}$. We find that J_{1c} only receives generically unsuppressed contributions,

$$\begin{aligned} J_{1c} = {} & \frac{3}{2}\rho_1 f_0^2 + 3N^2(|\Delta_S|^2 + |\Delta_P|^2)\frac{\lambda}{m_b^2}A_0^2 \\ & + \mathcal{O}(m_\ell^2/q^2, m_s/m_b)\,. \end{aligned} \tag{45}$$

Helicity-suppressed ($\sim m_\ell/\sqrt{q^2}$) contributions from interference terms SM $\times$ S arise in $J_{5,6c,7}$. For the explicit expressions see Appendix B.

We find that in the presence of (S+P) operators the low recoil relations

$$|H_T^{(1)}| = 1\,, \qquad H_T^{(1b)} = 1 + \mathcal{O}\left(\frac{m_\ell}{\sqrt{q^2}}\right), \qquad H_T^{(4)} = H_T^{(5)} \tag{46}$$

hold, and $H_T^{(3,4,5)}$ remain long-distance free. Since $J_{8,9}$ vanish in the considered scenario $H_T^{(4)} = H_T^{(5)} = 0$, and $H_T^{(1c)}$ is ill-defined as in the SM-like scenario.

The helicity-suppressed contributions to J_5 break the relation $H_T^{(2)} = H_T^{(3)}$ at $\mathcal{O}(m_\ell/\sqrt{q^2})$ through a finite Δ_S. In this case $H_T^{(2)}$ ceases to be free of form factors, and rather depends on A_0/f_0. Moreover, the relation $J_7 = 0$ is broken at $\mathcal{O}(m_\ell/\sqrt{q^2})$ if there is additionally CP violation beyond the SM. With the exception of using J_5, the ratio $f_0/f_\parallel$ can be extracted by means of the methods proposed in Eqs. (17) and (41).

The (pseudo-)scalar contributions to J_{1c} break the relation $J_{1c} = -J_{2c}$, valid only in the (SM+SM') basis for $m_\ell \to 0$, see also Appendix B. At the same time, contributions to the longitudinal polarization F_L of K^* mesons are induced, see Eq. (A9). These contributions prohibit that F_L and $A_{\rm FB}$, the lepton forward-backward asymmetry, can be extracted simultaneously from a fit to Eq. (A11), the angular distribution in $\cos\theta_\ell$. Note that F_L and $F_T = 1 - F_L$ can be extracted from Eq. (A8), the distribution in $\cos\theta_K$, in a model-independent way. Discrepancies between the extracted values of $F_{L,T}$ from Eqs. (A8) and (A11) would indicate BSM physics. (We assume here that S-wave contributions from $\bar{B} \to \bar{K}\pi\ell^+\ell^-$ have been removed from the data, see Section VI B.) Note also that interference terms (SM+SM') $\times$ S contribute to $A_{\rm FB}$ via J_{6c} due to (A7).

D. Tensor operators

The tensor operators (T+T5) give rise to additional tensor transversity amplitudes A_{ij}. Here the labels i and j denote the transversity state $t, \perp, \parallel, 0$ of the polarization vectors which comprise the rank-two polarization tensor that was used in the computation. We obtain for pairs $(\parallel\perp,\, t0)$, $(0\,\perp,\, t\,\perp)$, $(0\,\parallel,\, t\,\parallel)$ the total angular momenta $J = 0, 1, 2$, respectively. For the definition of the transversity amplitudes and their general results, see Appendix C and Eqs. (B18)-(B20), respectively.

At low recoil, after application of the improved Isgur-Wise relations, we obtain

$$\begin{aligned} A_{\parallel\perp,\,t0} &= \pm\mathcal{C}_{T,\,T5}\,\frac{2\kappa}{\sqrt{q^2}} M_B(1+\hat\Lambda_0) f_0\,, \\ A_{t\perp,\,0\perp} &= \pm\mathcal{C}_{T,\,T5}\,\frac{\sqrt{2}\kappa}{\sqrt{q^2}} M_B(1+\hat\Lambda_\perp)\, f_\perp\,, \\ A_{0\parallel,\,t\parallel} &= \pm\mathcal{C}_{T,\,T5}\,\frac{\sqrt{2}\kappa}{\sqrt{q^2}} M_B(1+\hat\Lambda_\parallel)\, f_\parallel\,, \end{aligned} \tag{47}$$

where $\hat\Lambda_{0,\perp,\parallel} = \mathcal{O}\left(\Lambda_{\rm QCD}/M_B\right)$ and the upper and lower sign refers to C_T and C_{T5}, respectively.

In the presence of tensor operators T and T5 in addition to (SM + SM') the angular observables J_i receive *i)* contributions which do not interfere with other operators in $J_{1s,1c,2s,2c,3,4}$, and *ii)* helicity-suppressed interference contributions in $J_{1s,1c,5,6s,6c,7}$, and *iii)* no contributions in $J_{8,9}$ from the additional six transversity amplitudes $A_{t0,\,\parallel\perp,\,t\perp,\,t\parallel,\,0\perp,\,0\parallel}$. We find

$$\begin{aligned} \frac{8}{3}J_{1s} &= \Big[3\rho_1^+ + \rho_1^T\,(1+\hat\Lambda_\perp)^2\Big] f_\perp^2 \\ &\quad + \Big[3\rho_1^- + \rho_1^T\,(1+\hat\Lambda_\parallel)^2\Big] f_\parallel^2 + \mathcal{O}\left(\frac{m_\ell}{\sqrt{q^2}}\right), \\ \frac{4}{3}J_{1c} &= 2\left[\rho_1^- + \rho_1^T\,(1+\hat\Lambda_0)^2\right] f_0^2 + \mathcal{O}\left(\frac{m_\ell}{\sqrt{q^2}}\right), \\ \frac{4}{3\beta_\ell^2}(2J_{2s} \pm J_3) &= 2\Big[\rho_1^\pm - \rho_1^T\,(1+\hat\Lambda_{\perp,\parallel})^2\Big] f_{\perp,\,\parallel}^2\,, \\ -\frac{4}{3\beta_\ell^2}J_{2c} &= 2\Big[\rho_1^- - \rho_1^T\,(1+\hat\Lambda_0)^2\Big] f_0^2\,, \\ \frac{4\sqrt{2}}{3\beta_\ell^2}J_4 &= 2\Big[\rho_1^- - \rho_1^T\,(1+\hat\Lambda_0)(1+\hat\Lambda_\parallel)\Big] f_0 f_\parallel\,, \\ \frac{2\sqrt{2}}{3\beta_\ell}J_5 &= 4\,\mathrm{Re}\,(\rho_2)\, f_0 f_\perp + \mathcal{O}\left(\frac{m_\ell}{\sqrt{q^2}}\right), \\ \frac{2}{3\beta_\ell}J_{6s} &= 4\,\mathrm{Re}\,(\rho_2)\, f_\parallel f_\perp + \mathcal{O}\left(\frac{m_\ell}{\sqrt{q^2}}\right), \\ J_{6c,7} &= \mathcal{O}\left(\frac{m_\ell}{\sqrt{q^2}}\right), \\ \frac{4\sqrt{2}}{3\beta_\ell^2}J_8 &= 4\,\mathrm{Im}\,(\rho_2)\, f_0 f_\perp\,, \\ -\frac{4}{3\beta_\ell^2}J_9 &= 4\,\mathrm{Im}\,(\rho_2)\, f_\parallel f_\perp\,. \end{aligned} \tag{48}$$

Here the additional short-distance combination reads

$$\rho_1^T \equiv 16\,\kappa^2\,\frac{M_B^2}{q^2}\Big(|\mathcal{C}_T|^2 + |\mathcal{C}_{T5}|^2\Big)\,. \tag{49}$$

Without tensor operators the ratio $H_T^{(1)}$ is free of short- and long-distance contributions. In the presence of the

tensor operators we obtain

$$H_T^{(1)} = \mathrm{sgn}(f_0)\,\mathrm{sgn}(\rho_1^- - \rho_1^T) \times \left[1 + \frac{\rho_1^-\,\rho_1^T}{2(\rho_1^- - \rho_1^T)^2}\left(\hat\Lambda_0 - \hat\Lambda_\parallel\right)^2\right] + \mathcal{O}\left(\hat\Lambda_i^3\right) \tag{50}$$

and form factor factors still cancel. Deviations from $|H_T^{(1)}| = 1$ arise at $\mathcal{O}(\hat\Lambda_i^2)$, while in $H_T^{(1b,\,1c)}$ the suppression is only linear in $\hat\Lambda_i$. For instance,

$$H_T^{(1b)} = 1 - \frac{\rho_1^T}{\rho_1^- - \rho_1^T}(\hat\Lambda_0 - \hat\Lambda_\parallel) + \mathcal{O}\left(\hat\Lambda_i^2\right). \tag{51}$$

We further find that in scenarios with tensor operators $H_T^{(3,4,5)}$ remain free of hadronic form factors, and the relations $H_T^{(2)}/H_T^{(3)} = 1$ and $H_T^{(4)}/H_T^{(5)} = 1$ hold up to helicity-suppressed and power-suppressed terms, respectively, see Table I and II.

The relation $J_{1c} + J_{2c} = 0$, valid in the (SM+SM') for $m_\ell \to 0$, is broken by ρ_1^T

$$J_{1c} + J_{2c} = 3\,\rho_1^T\,(1+\hat\Lambda_0)^2 f_0^2 + \mathcal{O}\left(\frac{m_\ell}{\sqrt{q^2}}\right). \tag{52}$$

E. Interference between operator sets

When considering the complete set of $|\Delta B| = |\Delta S| = 1$ semileptonic operators, all of the previously presented low recoil relations are broken at some level, which can however be parametrically suppressed and small. For instance, the relations $H_T^{(2)}/H_T^{(3)} = 1$ and $J_7 = 0$ are broken at leading order by the simultaneous presence of tensors and scalars only, while $H_T^{(4)}/H_T^{(5)} = 1$ remains intact up to $\mathcal{O}(\hat\Lambda_i)$-suppressed terms, see Table I for an overview.

The angular observables J_{1c}, J_5, J_{6c} and J_7 receive contributions from (pseudo-) scalar operators involving the form factor A_0, see Section III C. These terms modify the otherwise general structure

$$J_a \sim \rho_i\, f_k f_l\,. \tag{53}$$

Corrections to J_{1c} arise from operators S and P, while J_5, J_{6c} and J_7 are modified by interferences of S and P with tensor operators.

Since the angular observables $J_{2s,2c,3,4,6s,8,9}$ obey Eq. (53) it follows that $H_T^{(1,3,4,5)}$ remain free of hadronic inputs in the complete operator basis. Our findings are summarized in Table II.

IV. $\bar B \to \bar K \ell^+\ell^-$ AT LOW RECOIL

The decay $\bar B \to \bar K \ell^+\ell^-$ is another accessible FCNC channel, which depends on the Wilson coefficients in a complementary way to $\bar B \to \bar K^*\ell^+\ell^-$. The angular distribution of $\bar B \to \bar K \ell^+\ell^-$ can be written as

$$\frac{d^2\Gamma^K}{dq^2 d\cos\theta_\ell} = a + b\,\cos\theta_\ell + c\,\cos^2\theta_\ell\,, \tag{54}$$

where the angle θ_ℓ is defined as in $\bar B \to \bar K^*\ell^+\ell^-$ decays, see Appendix A. The q^2-dependent coefficients a, b and c are related to the decay rate, the lepton forward-backward asymmetry, $A_{\rm FB}^K$, and the flat term, F_H, as follows [19]

$$\begin{aligned} \frac{d\Gamma^K}{dq^2} &= 2\,(a + c/3)\,, \\ A_{\rm FB}^K &= \frac{b}{d\Gamma/dq^2}\,, \qquad F_H = \frac{2\,(a+c)}{d\Gamma/dq^2}\,. \end{aligned} \tag{55}$$

Here we label the $\bar B \to \bar K \ell^+\ell^-$decay rate and forward-backward asymmetry by a superscript 'K' to distinguish them from the ones in $\bar B \to \bar K^*\ell^+\ell^-$ decays.

Similar to $\bar B \to \bar K^*\ell^+\ell^-$ the low recoil OPE and the Isgur-Wise relations can be applied, allowing to trade the $B \to K$ tensor form factor f_T for the vector one f_+ [2, 28]. We obtain for the extended operator basis at low recoil to leading order in $1/m_b$

$$\frac{4\,a}{\Gamma_0\sqrt{\lambda_0}^3 f_+^2} = \rho_1^+ + \frac{f_0^2}{f_+^2}\rho^{S+P} + \frac{m_\ell}{M_B}\rho^{T\times 79} + \frac{m_\ell}{\sqrt{q^2}}\frac{f_0^2}{f_+^2}\rho^{P\times 10}\,, \tag{56}$$

$$\frac{b}{\Gamma_0\lambda_0(M_B^2 - M_K^2)f_+ f_0} = \rho^{S\times T + P\times T5} + \frac{m_\ell}{\sqrt{q^2}}\rho^{T5\times 10} + \frac{m_\ell}{m_b - m_s}\rho^{S\times 79}\,, \tag{57}$$

$$\frac{4\,c}{\Gamma_0\sqrt{\lambda_0}^3 f_+^2} = -\rho_1^+ + \rho_1^T\,, \tag{58}$$

where $\lambda_0 \equiv \lambda(M_B^2, M_K^2, q^2)$ and

$$\rho^{S+P} \equiv \frac{q^2(M_B^2 - M_K^2)^2}{(m_b - m_s)^2\lambda_0} \times \left(|\mathcal{C}_S + \mathcal{C}_{S'}|^2 + |\mathcal{C}_P + \mathcal{C}_{P'}|^2\right), \tag{59}$$

$$\rho^{P\times 10} \equiv \frac{\sqrt{q^2}}{(m_b - m_s)}\frac{(M_B^2 - M_{K^*}^2)^2}{\lambda_0} \times 4\,\mathrm{Re}\left[(\mathcal{C}_P + \mathcal{C}_{P'})\,(\mathcal{C}_{10} + \mathcal{C}_{10'})^*\right], \tag{60}$$

$$\rho^{T\times 79} \equiv 16\,\kappa\frac{M_B^2}{q^2}\,\mathrm{Re}\left[\mathcal{C}_T\left(\mathcal{C}_{79}^{\rm eff} + \mathcal{C}_{7'9'}^{\rm eff}\right)^*\right], \tag{61}$$

$$\rho^{S\times T + P\times T5} \equiv 2\,\kappa\frac{M_B}{m_b - m_s} \times \mathrm{Re}\left[(\mathcal{C}_S + \mathcal{C}_{S'})\,\mathcal{C}_T^* + (\mathcal{C}_P + \mathcal{C}_{P'})\,\mathcal{C}_{T5}^*\right], \tag{62}$$

$$\rho^{T5\times 10} \equiv 4\,\kappa\frac{M_B}{\sqrt{q^2}}\,\mathrm{Re}\left[(\mathcal{C}_{10} + \mathcal{C}_{10'})\,\mathcal{C}_{T5}^*\right], \tag{63}$$

$$\rho^{S\times 79} \equiv \mathrm{Re}\left[(\mathcal{C}_S + \mathcal{C}_{S'})\left(\mathcal{C}_{79}^{\rm eff} + \mathcal{C}_{7'9'}^{\rm eff}\right)^*\right]. \tag{64}$$

Scenario	$\lvert H_T^{(1)}\rvert = 1$	$H_T^{(2)} = H_T^{(3)}$	$H_T^{(4)} = H_T^{(5)}$	$J_{6c} = 0$	$J_7 = 0$	$J_{8,9} = 0$
SM	✓	✓	(✓)	✓	✓	✓
SM + (S+P)	✓	$\frac{m_\ell}{Q}\,\mathrm{Re}\,(\mathcal{C}_{79}\Delta_S^*)$	(✓)	$\frac{m_\ell}{Q}\,\mathrm{Re}\,(\mathcal{C}_{79}\Delta_S^*)$	$\frac{m_\ell}{Q}\,\mathrm{Im}\,(\mathcal{C}_{79}\Delta_S^*)$	✓
SM + (T+T5)	$\frac{\Lambda^2}{Q^2}\rho_1^T$	$\frac{m_\ell}{Q}\,\mathrm{Re}\,\big(\mathcal{C}_{10}\mathcal{C}_{T(T5)}^*\big)$	(✓)	$\frac{m_\ell}{Q}\,\mathrm{Re}\,(\mathcal{C}_{10}\mathcal{C}_T^*)$	$\frac{m_\ell}{Q}\,\mathrm{Im}\,(\mathcal{C}_{10}\mathcal{C}_{T5}^*)$	✓
SM + SM'	✓	✓	✓	✓	✓	$\mathrm{Im}\,(\rho_2)$
all	$\frac{\Lambda^2}{Q^2}\rho_1^T$	$\mathrm{Re}\,\big(\mathcal{C}_{T(T5)}\Delta_{P(S)}^*\big)$	$\frac{\Lambda}{Q}\,\rho_1^T\,\mathrm{Im}\,(\rho_2)$	$\mathrm{Re}\,\big(\mathcal{C}_{T(T5)}\Delta_{P(S)}^*\big)$	$\mathrm{Im}\,\big(\mathcal{C}_{T(T5)}\Delta_{S(P)}^*\big)$	$\mathrm{Im}\,(\rho_2)$

TABLE I: The low recoil relations in SM-like models (first row) and the leading terms that break them in SM extensions. A ✓denotes at most corrections of order α_s/m_b and $\mathcal{C}_7/(\mathcal{C}_9 m_b)$. A (✓) reminds that up to the latter corrections $H_T^{(4,5)} = 0$. Here $\Lambda = \Lambda_{\rm QCD}$, $Q = \mathcal{O}(m_b, \sqrt{q^2})$ and $\Delta_{S,P} \equiv C_{S,P} - C_{S',P'}$, for details see text.

Scenario	$H_T^{(1)}$	$H_T^{(2)}$	$H_T^{(3)}$	$H_T^{(4)}$	$H_T^{(5)}$
SM	✓	✓	✓	—	—
SM + (S+P)	✓	A_0	✓	—	—
SM + (T+T5)	✓	✓	✓	✓	✓
SM + SM'	✓	✓	✓	✓	✓
all	✓	A_0	✓	✓	✓

TABLE II: The low recoil observables $H_T^{(i)}$, and the degree to which they remain free of hadronic input. A ✓denotes at most corrections of order α_s/m_b and $\mathcal{C}_7/(\mathcal{C}_9 m_b)$, while A_0 denotes breaking through terms involving the corresponding $B \to K^*$ form factor. Observables marked with — vanish in the considered scenario.

Here we have neglected terms suppressed by m_ℓ^2/M_B^2, but kept those proportional to $m_\ell/\sqrt{q^2}$. The form factor f_+ and the scalar one f_0, as well as the normalization Γ_0 are defined in [19, 28], whereas ρ_1^+ and ρ_1^T have been introduced in Section III.
In the scenario (SM+SM') the differential decay rate

$$\frac{d\Gamma^K}{dq^2} = \Gamma_0 \frac{\sqrt{\lambda_0}^3}{3} f_+^2\, \rho_1^+ \,, \tag{65}$$

yields a complementary constraint on ρ_1^+. The CP asymmetry of the rate, $A_{\rm CP}$, turns out to be free of long distance uncertainties, as f_+ cancels, and the CP asymmetries

$$A_{\rm CP}[\bar B \to \bar K \ell^+\ell^-] = a_{\rm CP}^{(1,+)}[\bar B \to \bar K^* \ell^+\ell^-] \tag{66}$$

in $\bar B \to \bar K \ell^+\ell^-$ and $\bar B \to \bar K^* \ell^+\ell^-$ decays are identical at low recoil, see Eq. (40). The equality Eq. (66) allows to measure CP violation with the combined, larger data set. If the CP asymmetries turn out to be not equal it would imply contributions from outside of (SM+SM').
Furthermore, the decay $\bar B \to \bar K \ell^+\ell^-$ provides with F_H a powerful observable, which exhibits sensitivity to (S+P) and (T+T5) operators, whereas the (SM+SM') contributions are suppressed by m_ℓ^2/q^2 [19],

$$F_H = \frac{3}{2} \cdot \frac{\rho_1^T + \frac{f_0^2}{f_+^2}\rho^{S+P}}{\rho_1^+ + \frac{1}{2}\rho_1^T + \frac{3}{2}\frac{f_0^2}{f_+^2}\rho^{S+P}} + \mathcal{O}\left(m_\ell/M_B\right) . \tag{67}$$

While the terms of $\mathcal{O}\left(m_\ell/M_B\right)$ in the denominator might be safely neglected in view of the numerically leading term ρ_1^+, they could become of some relevance in the numerator of F_H if ρ_1^T and/or ρ^{S+P} are small and the interference of $\mathcal{C}_T$ and/or $\mathcal{C}_{P^{(\prime)}}$ with the large (SM+SM') contributions can overcome the lepton mass suppression. The importance of the flat term in SM tests and NP searches becomes manifest from Eq. (67) since F_H is given directly by the magnitude of scalar and tensor Wilson coefficients and secondly it depends only on form factor ratios rather than the form factors themselves. For tensor contributions, this residual dependence drops out and F_H is free of hadronic uncertainties.
On the other hand, in $A_{\rm FB}^K$ tensor and (pseudo-)scalar operators need to be either simultaneously present or their contributions are lepton-mass suppressed, such as the interference terms between SM(') and T,T5,S, and P. Moreover, $A_{\rm FB}^K$ depends on the ratio of form factors f_0/f_+. We obtain

$$A_{\rm FB}^K = \frac{3(M_B^2 - M_K^2)}{\sqrt{\lambda_0}} \frac{f_0}{f_+} \frac{\rho^{S\times T+P\times T5}}{\rho_1^+ + \frac{1}{2}\rho_1^T + \frac{3}{2}\frac{f_0^2}{f_+^2}\rho^{S+P}} + \mathcal{O}\left(m_\ell/M_B\right) . \tag{68}$$

V. SENSITIVITY TO NEW PHYSICS

The fact that no order one NP signals have been observed in (semi)leptonic $|\Delta B| = 1$ processes to date suggests that NP effects with the exception of null tests are suppressed with respect to the SM contributions. Good control of theoretical uncertainties is therefore crucial to progress.

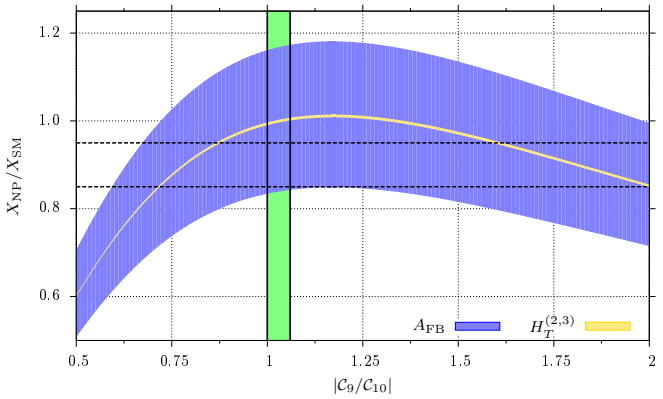

FIG. 2: The sensitivity of $A_{\rm FB}$ (blue shaded band) and $H_T^{(2,3)}$ (thin gold shaded band) to $|\mathcal{C}_9/\mathcal{C}_{10}|$ normalized to their respective SM values and in the low recoil bin $14.18\,\text{GeV}^2 \leq q^2 \leq 19.21\,\text{GeV}^2$. The dashed horizontal black lines indicate hypothetical measurements at $(90 \pm 5)\%$, while the vertical green band shows $|\mathcal{C}_9/\mathcal{C}_{10}|$ in the SM.

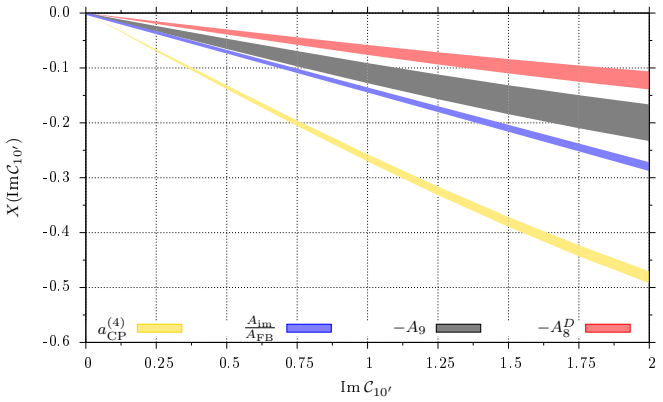

FIG. 3: The sensitivity of $a_{\rm CP}^{(4)}$, $A_{\rm im}/A_{\rm FB}$, $-A_9$ and $-A_8^D$ (from bottom to top) to $\text{Im}\,(\mathcal{C}_{10'})$ in the low recoil bin $14.18\,\text{GeV}^2 \leq q^2 \leq 19.21\,\text{GeV}^2$. All other NP couplings including $\text{Re}\,(\mathcal{C}_{10'})$ are set to zero.

Here we study the sensitivity of $\bar{B} \to \bar{K}^* \ell^+ \ell^-$ observables at low recoil. We demonstrate the advantages of the optimized low recoil observables $H_T^{(i)}$ and related CP asymmetries. For numerical input, see Appendix D.

We begin studying the sensitivity of $H_T^{(2,3)}$ versus $A_{\rm FB}$ to $\mathcal{C}_{9,10}$ within the SM operator basis, where [4]

$$H_T^{(2,3)} = 2\,\frac{\rho_2}{\rho_1}\,, \tag{69}$$

$$A_{\rm FB} = 3\,\frac{\rho_2}{\rho_1}\,\frac{f_\perp f_\parallel}{(f_\perp^2 + f_\parallel^2 + f_0^2)}\,, \tag{70}$$

and

$$\frac{\rho_2}{\rho_1} \sim \frac{r}{1+|r|^2}\,, \qquad r = \frac{\mathcal{C}_9}{\mathcal{C}_{10}}\,, \tag{71}$$

and $r_{\rm SM} = -1.03 \pm 0.03$.

In Fig. 2 we show $H_T^{(2,3)}$ and $A_{\rm FB}$ integrated in the low recoil bin $14.18\,\text{GeV}^2 \leq q^2 \leq 19.21\,\text{GeV}^2$ versus $|\mathcal{C}_9/\mathcal{C}_{10}|$ and normalized to their SM values within their respective theory uncertainties. As can be seen, a hypothetical measurement of $A_{\rm FB}$ as good as $(90 \pm 5)\,\%$ (horizontal dashed black lines) would not be able to distinguish the SM from NP, due to the theory uncertainty. The latter is dominated by the one of the form factors, which only partially cancel within $A_{\rm FB}$. Given our current understanding of the $B \to K^*$ form factors, an experimental determination of $A_{\rm FB}$ in the low recoil region that strives to indicate NP must exclude values larger than $0.85 \times A_{\rm FB}^{\rm SM}$ and lower than $1.18 \times A_{\rm FB}^{\rm SM}$. On the other hand, the $(90 \pm 5)\,\%$ measurement in $H_T^{(2)}$ or $H_T^{(3)}$ would suffice to establish NP due to the small, subpercent level theoretical uncertainty [4]. An advanced few percent-level measurement would probe $|\mathcal{C}_9/\mathcal{C}_{10}|$ up to a discrete ambiguity at similar, few percent level.

In Fig. 3 we show the q^2-integrated observables $A_{\rm im}/A_{\rm FB} = J_9/J_{6s}$, $a_{\rm CP}^{(4)}$, $-A_8^D$ and $-A_9$ for $14.18\,\text{GeV}^2 \leq q^2 \leq 19.21\,\text{GeV}^2$. For the definition of A_8^D, A_9, see [7]. All observables are shown as functions of the (imaginary part of the) NP coupling $\text{Im}\,(\mathcal{C}_{10'})$. All other NP Wilson coefficients including $\text{Re}\,(\mathcal{C}_{10'})$ are assumed to be zero. Since the observables are odd functions of $\text{Im}\,(\mathcal{C}_{10'})$ to a very high degree the values for $\text{Im}\,(\mathcal{C}_{10'}) < 0$ are not shown.

We find that $A_{\rm im}/A_{\rm FB}$ as well as $a_{\rm CP}^{(4)}$ are better suited to probe small values of $\text{Im}\,(\mathcal{C}_{10'})$ due to their steeper slope and smaller relative theoretical uncertainties. Approximately (see Eq. (A2) for $\langle\rangle$-notation),

$$\left\langle A_8^D \right\rangle \simeq (+0.061 \pm 0.008)\,\text{Im}\,(\mathcal{C}_{10'})\,, \tag{72}$$

$$\langle A_9 \rangle \simeq (+0.10 \pm 0.02)\,\text{Im}\,(\mathcal{C}_{10'})\,, \tag{73}$$

$$\langle A_{\rm im} \rangle \,/\, \langle A_{\rm FB} \rangle \simeq (-0.140 \pm 0.004)\,\text{Im}\,(\mathcal{C}_{10'})\,, \tag{74}$$

$$\left\langle a_{\rm CP}^{(4)} \right\rangle \simeq (-0.240 \pm 0.005)\,\text{Im}\,(\mathcal{C}_{10'})\,, \tag{75}$$

where we estimated the theory uncertainty from residual $1/m_b$ corrections and form factors similar to [5]. Note that both $A_{\rm im}$ and $A_{\rm FB}$ have been separately measured by CDF in two low recoil bins [29]. Due to the current experimental uncertainties and the absence of information on the correlation of the individual errors we refrain from calculating the ratio.

VI. PROBING THE OPE

The relations between the low recoil observables can be used to quantitatively test the performance of the OPE. We employ the following ansatz:

$$A_i^{L,R} \propto C^{L,R}\, f_i(1+\epsilon_i)\,, \qquad i = \perp, \parallel, 0\,. \tag{76}$$

Here the terms ϵ_i parametrize effects beyond Eq. (1) to each transversity state. These include higher order power corrections or contributions from even beyond the OPE

such as duality violation. There are no separate corrections for the left- and right-handed lepton chiralities as the photon-current as a mediator of the considered effects couples vectorlike. Although not explicitly written the ϵ_i are in general q^2-dependent. Our ansatz parametrizes the most general situation within the SM neglecting lepton mass corrections of order m_ℓ^2/q^2.

The generic size of the subleading $1/m_b$ corrections imply ϵ_i of the order $\alpha_s\Lambda/m_b$ or $\mathcal{C}_7/\mathcal{C}_9\,\Lambda/m_b$, about few percent. This is taken into account in current uncertainty budgets [5]. It is therefore desirable to have sensitivity to corrections at the (few) percent level. On the other hand, it is hard to quantify duality violation. While in a toy model duality violating contributions have been estimated to be very small [2] it is nevertheless useful to have experimental checks.

We find that the corrections enter the short-distance and form factor free relations quadratically

$$\left\{|H_T^{(1)}|, \quad H_T^{(1b)}, \quad \frac{H_T^{(2)}}{H_T^{(3)}}\right\} = 1 + \mathcal{O}\left(\epsilon^2\right), \tag{77}$$

and the form factor ratios f_i/f_k linearly. The null tests depend linearly on the imaginary parts

$$J_{7,8,9} = \mathcal{O}\left(\mathrm{Im}(\epsilon)\right), \tag{78}$$

while the real parts enter at second order only. Note that the corrections Eq. (77) vanish for $\mathrm{Im}(\epsilon_i) = 0$ since for all ϵ_i real the ansatz Eq. (76) would correspond to a mere rescaling of the form factors.[1]

The double suppression in Eq. (77) makes these observables sensitive to somewhat sizable effects only or requires high experimental precision: For $\epsilon \sim 30\,(10)\,\%$ the correction amounts to about $10\,(1)\,\%$. On the other hand, the respective background from the SM OPE is at the permille level.

Due to the linear dependence and the generic appearance of unsuppressed strong phases in the nonperturbative regime we find that the null tests Eq. (78) have potentially higher sensitivity to OPE corrections. Up to $\mathcal{O}\left(\epsilon^2\right)$-corrections

$$J_7^\epsilon = -3\sqrt{2}\,\beta_\ell\,\rho_2\,f_0 f_\parallel\,\mathrm{Im}\left(\epsilon_0 - \epsilon_\parallel\right), \tag{79}$$

$$J_8^\epsilon = \frac{3}{2\sqrt{2}}\beta_\ell^2\rho_1 f_0 f_\perp \mathrm{Im}\left(\epsilon_0 - \epsilon_\perp\right), \tag{80}$$

$$J_9^\epsilon = \frac{3}{2}\beta_\ell^2\rho_1 f_\parallel f_\perp \mathrm{Im}\left(\epsilon_\perp - \epsilon_\parallel\right). \tag{81}$$

All coefficients in front of the imaginary parts are parametrically unsuppressed in the angular distribution.

We investigate corrections from NP in Section VI A and comment on an experimental background from $K\pi$ in an S-wave with invariant mass around the $K^*(892)$ mass in Section VI B.

[1] We thank the unknown referee for emphasizing this point.

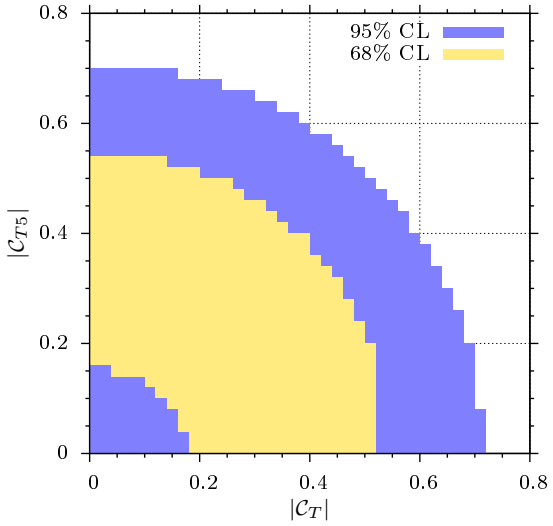

FIG. 4: The constraints on $|\mathcal{C}_T|$ and $|\mathcal{C}_{T5}|$ from $\bar{B} \to \bar{K}\ell^+\ell^-$ low recoil data at 68% CL (inner gold area) and 95% CL (outer blue areas).

A. NP pollution

As summarized in Table I, beyond the SM deviations from $|H_T^{(1)}| = 1$ arise from tensor operators only. Here we estimate their contributions allowing for complex Wilson coefficients. The currently strongest constraints stem from $\bar{B} \to \bar{K}\ell^+\ell^-$ decays, discussed in Section IV. We employ the recent LHCb measurements [30] of the branching ratio and the flat term F_H Eq. (67), combined with branching ratio measurements from Belle [31], BaBar [32] and CDF [33]. In the scenario (T+T5+SM+SM') we find at 95 % CL

$$|\mathcal{C}_T|^2 + |\mathcal{C}_{T5}|^2 \lesssim 0.5\,. \tag{82}$$

The bound is dominated by the LHCb measurement of the two highest q^2-bins of F_H. We recall that in F_H the form factor uncertainties drop out at leading order in this kinematic regime.

The outcome of our scan leading to Eq. (82) is shown in Fig. 4. Values of both $|\mathcal{C}_T|, |\mathcal{C}_{T5}|$ near zero are disfavored at 68 % CL. This follows from the current low recoil data on F_H [30], which have central values at $\sim 1\sigma$ above the SM.

Using Eqs. (49), (50) and (82) we obtain

$$\left||H_T^{(1)}| - 1\right| \lesssim 0.08\,. \tag{83}$$

Scalar and pseudo-scalar operators contribute predominantly constructively to F_H, such that they do not invalidate an upper bound on the tensor contributions.

The relation $H_T^{(2)}/H_T^{(3)} = 1$ receives corrections by the simultaneous presence of tensor and scalar operators, see Table I. The latter are constrained by $\bar{B}_s \to \mu^+\mu^-$ decays. Assuming that the branching ratio $\mathcal{B}(\bar{B}_s \to \mu^+\mu^-)$

is saturated by scalar operators $\mathcal{O}_{S^{(\prime)}}$ we find $|\Delta_S| \lesssim 0.59$ from the most recent upper bound $\mathcal{B}(\bar{B}_s \to \mu^+\mu^-) < 4.2\times 10^{-9}$ at 95 % CL [34]. For this bound we also consider B_s–$\bar{B}_s$ mixing effects pointed out in Ref. [35], allowing for $\mathcal{A}_{\Delta\Gamma} = -1$ and use $y_s = 0.088 \pm 0.014$. In combination with the bounds on the tensor couplings we obtain

$$|H_T^{(2)}/H_T^{(3)} - 1| \lesssim 0.12\,\text{GeV} \times N\frac{f_\parallel A_0}{f_\perp f_0} \simeq 0.06\,. \qquad (84)$$

Subleading effects from scalar operators alone are suppressed by m_ℓ/Q and do not exceed the percent level for muons.

The relation $J_7 = 0$ receives corrections from NP with either m_ℓ/Q-suppression or require tensor contributions. To estimate the sensitivity to OPE corrections vs. NP we compare the respective contributions

$$\frac{J_7^{\rm NP}}{J_7^\epsilon} \simeq 2\frac{\sqrt{\lambda}}{\sqrt{q^2}}\,\frac{\text{Im}\left(\mathcal{C}_T\Delta_S^* + \mathcal{C}_{T5}\Delta_P^*\right)}{\rho_2 \text{Im}\left(\epsilon_0 - \epsilon_\parallel\right)}\,N\frac{A_0 f_\perp}{f_0 f_\parallel} \qquad (85)$$

$$\lesssim \left(\frac{0.04}{\text{Im}\left(\epsilon_0 - \epsilon_\parallel\right)}\right)\,. \qquad (86)$$

We learn that J_7 probes the OPE as good as at the few percent level, before tensor induced contributions can keep up. NP contributions to J_7 from scalar operators interfering with the SM are suppressed by m_ℓ/Q, which do not exceed the percent level for muons.

We further find that both J_8 and J_9 are more sensitive to NP than J_7, with similar sensitivities given as

$$\frac{J_8^{\rm NP}}{J_8^\epsilon} \simeq \frac{2\,\text{Im}\left(\rho_2\right)}{\rho_1 \text{Im}\left(\epsilon_0 - \epsilon_\perp\right)}\,, \qquad (87)$$

$$\frac{J_9^{\rm NP}}{J_9^\epsilon} \simeq \frac{-2\,\text{Im}\left(\rho_2\right)}{\rho_1 \text{Im}\left(\epsilon_\perp - \epsilon_\parallel\right)}\,, \qquad (88)$$

both of which are generically order one in the presence of order one CP phases, see Eq. (35), unless the ϵ_i are $\mathcal{O}(1)$ or larger. We conclude that J_8 and J_9 are likely to probe CP violating right-handed currents.

In general tensor operators are absent or small in most models; they arise *e.g.,* from box-type matching conditions, can contribute to Wilson coefficients of dipole operators via renormalization group mixing [36, 37] or arise in models with FCNC at tree-level, such as those with leptoquarks, as discussed in [19]. In this respect the OPE-based predictions of the short-distance independence of $H_T^{(1)}, H_T^{(2))}/H_T^{(3)}$ and J_7 are very clean.

B. S-wave pollution

We discuss the impact of the experimental background from $\bar{K}\pi$ in an S-wave on the $\bar{B} \to \bar{K}^*(\to \bar{K}\pi)\ell^+\ell^-$ angular analysis, recently addressed in Refs. [38–40] for the low q^2 region.

The resonant spin zero $\bar{K}\pi$-contributions barely affect the low recoil region as the masses of the well established scalar kaons, notably $K_0^*(1430)$ cause their kinematical endpoint $q^2_{\rm max} = 15\,\text{GeV}^2$ to have barely overlap with the low recoil bin $q^2 \gtrsim (14-15)\text{GeV}^2$ [38]. In addition there is already phase space suppression $\propto \lambda_0^{3/2}$ below the endpoint. A nonresonant contribution with invariant mass around m_{K^*} is, however, not suppressed by these arguments and can affect the required precision extraction of the angular observables J_i [40] for SM or OPE tests.

Fortunately all S-wave backgrounds can be controlled experimentally. The effect of an underlying spin zero component in the $\bar{B} \to \bar{K}^*(\to \bar{K}\pi)\ell^+\ell^-$ angular distribution Eq. (A1) can be parametrized as follows:

i) The J_i for $i = 3, 6, 9$ do not receive S-wave contributions.

ii) The terms $[J_i \sin 2\theta_K]$ for $i = 4, 5, 7, 8$ in Eq. (A1) need to be replaced by $[J_i \sin 2\theta_K + \tilde{J}_i \sin\theta_K]$. The $\tilde{J}_i$ denote interference terms; due to their different angular dependence they can be isolated.

iii) The terms $[J_{is}\sin^2\theta_K + J_{ic}\cos^2\theta_K]$ for $i = 1, 2$ in Eq. (A1) need to be replaced by $[(J_{is}+\tilde{J}_{is})\sin^2\theta_K + (J_{ic} + \tilde{J}_{ic})\cos^2\theta_K + \tilde{J}_{isc}\cos\theta_K]$. The interference terms $\tilde{J}_{isc}$ can be identified by angular analysis. The $\tilde{J}_{is}, \tilde{J}_{ic}$ stem from S-waves only and can be measured at invariant $\bar{K}\pi$ masses outside of the $K^*(892)$ peak, where the J_{is}, J_{ic} can be neglected.

Note that all $\tilde{J}_i$ depend in general on q^2; they incorporate resonant and nonresonant scalar contributions.

Procedure *iii)* is required for all $H_T^{(k)}$ as well as observables which are normalized to the rate. The accuracy to which the $\tilde{J}_{ix}$, $i = 1, 2, x = s, c$ can be measured limits the experimental precision on the J_{ix}. Note that $J_{7,8,9}$ and the observables given in Eq. (36) can be extracted without side-band measurements. J_9 and the second observable in Eq. (36), which is proportional to J_9/J_{6s} do not receive contributions from S-waves at all.

VII. CONCLUSIONS

We analyze $\bar{B} \to \bar{K}^*(\to \bar{K}\pi)\ell^+\ell^-$ and $\bar{B} \to \bar{K}\ell^+\ell^-$ decays, $\ell = e, \mu$, at low hadronic recoil in the most general basis of semileptonic dimension-six effective couplings. We investigate to which extent the beneficial features obtained from angular analysis and the OPE in the SM-like operator basis hold. We find:

The transversity observables $H_T^{(i)}$, $i = 1, 3, 4, 5$ remain in the general case free of hadronic matrix elements and are clean tests of the SM and beyond; for $H_T^{(2)}$ this is true if contributions from scalar operators are ignored, see Table II.

The form factor ratio $f_0/f_\parallel$ can be extracted by means of Eqs. (17) and (41), excluding methods based on J_5 if

scalar operators are present. If no chirality-flipped operators contribute the ratios Eqs. (18) and (19) allow for a short-distance free extraction of form factor ratios involving $f_\perp$. There is a residual short-distance dependence from tensor operators in Eq. (17), which, however, is $\Lambda_{\rm QCD}/M_B$ suppressed.

The low recoil relations among the $H_T^{(i)}$ and $J_{7,8,9} = 0$ receive corrections from both NP, see Table I, and contributions beyond the leading order OPE Eq. (1), as given in Eq. (76) and discussed in Section VI. Our analysis shows that with the present $|\Delta B| = |\Delta S| = 1$ constraints J_7 has model-independently the highest sensitivity to the latter corrections at the percent level, before a potential NP background kicks in. The sensitivity in $|H_T^{(1)}| = 1$ to OPE corrections becomes comparable or better if tensor operators are ignored. The interplay of constraints will evolve with future rare decay measurements, and the actual sensitivity to the OPE can increase.

The observables $J_{8,9}$ are sensitive to CP violating chirality-flipped contributions. We suggest to explore such scenarios with the observables $H_T^{(4,5)}$ and the respective CP- and T-odd CP asymmetry $a_{\rm CP}^{(4)}$, all of which vanish in the SM-like basis. Further null tests are the ratios Eq. (36). Note that one of the latter, $J_9/J_{6s} = A_{\rm im}/A_{\rm FB}$ has already been experimentally accessed [29].

Our findings are of direct use to the high statistics studies at the LHC(b) experiments and forthcoming high luminosity flavor factories. We look forward to this application and future data.

Acknowledgments

DvD is grateful to Sebastian Hollenberg for comments on the manuscript, and to the particle theory group at the Excellence Cluster "Origin and Structure of the Universe" for kind hospitality during which parts of this work have been completed. GH gratefully acknowledges the kind hospitality of the theory group at DESY Hamburg, where parts of this work have been done. We thank Roman Zwicky for useful communications.

Appendix A: Angular distribution

The differential decay rate of $\bar{B} \to \bar{K}^*(\to \bar{K}\pi)\,\ell^+\ell^-$ can, after summing over the lepton spins, assuming an on-shell $\bar{K}^*$ of narrow width, and integrating over the $\bar{K}\pi$-invariant mass, be written as

$$\begin{aligned}\frac{8\pi}{3}\frac{d^4\Gamma}{dq^2\, d\cos\theta_\ell\, d\cos\theta_K\, d\phi} =& \\ &(J_{1s} + J_{2s}\cos 2\theta_\ell + J_{6s}\cos\theta_\ell)\sin^2\theta_K \\ &+(J_{1c} + J_{2c}\cos 2\theta_\ell + J_{6c}\cos\theta_\ell)\cos^2\theta_K \\ &+(J_3\cos 2\phi + J_9\sin 2\phi)\sin^2\theta_K\sin^2\theta_\ell \\ &+(J_4\cos\phi + J_8\sin\phi)\sin 2\theta_K\sin 2\theta_\ell \\ &+(J_5\cos\phi + J_7\sin\phi)\sin 2\theta_K\sin\theta_\ell\,,\end{aligned} \tag{A1}$$

with twelve angular coefficients $J_i = J_i(q^2)$ times the angular dependence. The angles are defined as i) the angle θ_ℓ between ℓ^- and $\bar{B}$ in the $(\ell^+\ell^-)$ center of mass system (cms), ii) the angle θ_K between K^- and the negative direction of flight of the $\bar{B}$ in the $(K^-\pi^+)$ cms [2] and iii) the angle ϕ between the two decay planes spanned by the 3-momenta of the $(K^-\pi^+)$- and $(\ell^+\ell^-)$-systems, respectively [6–8, 16].
Within the (SM+SM') operator basis holds $J_{6c} = 0$. A nonvanishing J_{6c} arises only from interference between the operator sets (SM+SM') and S [8], (SM+SM') and T, and P and T [21]. The explicit expressions of the J_i are given in Appendix B.
We denote by

$$\langle J_i\rangle = \int_{q^2_{\rm min}}^{q^2_{\rm max}} dq^2\, J_i(q^2) \tag{A2}$$

q^2-integrated angular observables J_i in bins between $q^2_{\rm min}$ and $q^2_{\rm max}$. For composite observables X we use $\langle X\rangle = X(\langle J_i\rangle)$. We assume in the following that an S-wave background from $\bar{K}\pi$ around the $K^*(892)$ mass has been removed as discussed in Section VI B.
Starting from the q^2-integrated decay distribution $d^3\langle\Gamma\rangle/d\cos\theta_\ell\, d\cos\theta_K d\phi$ one obtains the integrated decay rate and the three single-angular differential distributions

$$\langle\Gamma\rangle = 2\langle J_{1s}\rangle + \langle J_{1c}\rangle - \frac{1}{3}\left(2\langle J_{2s}\rangle + \langle J_{2c}\rangle\right)\,, \tag{A3}$$

$$\frac{d\langle\Gamma\rangle}{d\phi} = \frac{\langle\Gamma\rangle}{2\pi} + \frac{2}{3\pi}\langle J_3\rangle\cos 2\phi + \frac{2}{3\pi}\langle J_9\rangle\sin 2\phi\,, \tag{A4}$$

$$\begin{aligned}\frac{d\langle\Gamma\rangle}{d\cos\theta_\ell} =& \langle J_{1s}\rangle + \frac{\langle J_{1c}\rangle}{2} + \left(\langle J_{6s}\rangle + \frac{\langle J_{6c}\rangle}{2}\right)\cos\theta_\ell \\ &+\left(\langle J_{2s}\rangle + \frac{\langle J_{2c}\rangle}{2}\right)\cos 2\theta_\ell\,,\end{aligned} \tag{A5}$$

[2] This corrects the *description* of θ_K as in v3 and earlier versions of this work, as well as Refs. [4, 5, 7]. De facto, in all of these works the description as spelled out here has already been used for all numerical and analytical studies, which explicitly includes the numerical implementation within EOS [45].

$$\frac{d\langle\Gamma\rangle}{d\cos\theta_K} = \frac{3}{2}\left[\left(\langle J_{1s}\rangle - \frac{1}{3}\langle J_{2s}\rangle\right)\sin^2\theta_K + \left(\langle J_{1c}\rangle - \frac{1}{3}\langle J_{2c}\rangle\right)\cos^2\theta_K\right] \tag{A6}$$

after integration over either all or the remaining two angles, respectively.
The lepton forward-backward asymmetry $A_{\rm FB}$ can be written as

$$\langle A_{\rm FB}\rangle\langle\Gamma\rangle = \langle J_{6s}\rangle + \frac{\langle J_{6c}\rangle}{2}\,, \tag{A7}$$

see Eq. (A5). The extraction of $J_{4,5,7,8}$ has been discussed in [7]. For alternative methods to obtain the J_i, see for example [8, 20, 39].
The longitudinal K^* polarization fraction F_L can model-independently be defined as

$$\frac{1}{\langle\Gamma\rangle}\frac{d\langle\Gamma\rangle}{d\cos\theta_K} = \frac{3}{4}\langle F_T\rangle\sin^2\theta_K + \frac{3}{2}\langle F_L\rangle\cos^2\theta_K\,. \tag{A8}$$

From comparison with Eq. (A6) one can read off

$$\langle F_L\rangle = \frac{1}{\langle\Gamma\rangle}\left(\langle J_{1c}\rangle - \frac{1}{3}\langle J_{2c}\rangle\right)\,, \tag{A9}$$

$$\langle F_T\rangle = \frac{2}{\langle\Gamma\rangle}\left(\langle J_{1s}\rangle - \frac{1}{3}\langle J_{2s}\rangle\right)\,, \tag{A10}$$

where $F_T + F_L = 1$.
In the experimental analyses by the collaborations Belle [31], BaBar [32], CDF [33] and LHCb [41] the distribution

$$\frac{1}{\langle\Gamma\rangle}\frac{d\langle\Gamma\rangle}{d\cos\theta_\ell} = \frac{3}{4}\langle F_L\rangle(1-\cos^2\theta_\ell) + \frac{3}{8}\langle F_T\rangle(1+\cos^2\theta_\ell) + \langle A_{\rm FB}\rangle\cos\theta_\ell \tag{A11}$$

is at least partially employed. We stress that the latter is based on [cf. Eqs. (B1) - (B4)]

$$J_{1s} = 3\,J_{2s}\,, \qquad J_{1c} = -J_{2c}\,, \tag{A12}$$

which is broken by $m_\ell \neq 0$ and/or in the presence of S, P, T or T5 contributions. Therefore, results for F_L based on Eq. (A11) do not hold in full generality.

Note that in cases where Eq. (A12) holds, such as the SM with lepton masses neglected, $F_L = (|A_0^L|^2 + |A_0^R|^2)/\Gamma = -J_{2c}/\Gamma$. Furthermore, $\langle J_{2s}\rangle = 3/16\,\langle\Gamma\rangle\,(1 - \langle F_L\rangle)$ and $\langle J_{2c}\rangle = -3/4\,\langle\Gamma\rangle\,\langle F_L\rangle$.

Appendix B: Angular observables

The $J_i(q^2)$ of Eq. (A1) can be conveniently expressed within the (SM+SM') operator basis with the help of seven transversity amplitudes, $A_{0,\perp,\parallel}^{L,R}$ and A_t, [6]. The operators S require an additional amplitude A_S, whereas the set P can be absorbed into the amplitude A_t [8]. In the presence of tensor operators T and T5, six additional transversity amplitudes A_{ij} need to be introduced, with $ij = \{\|\perp, t0, t\perp, t\|, 0\perp, 0\|\}$, see Appendix C. In the complete basis (SM+SM') + (S+P) + (T+T5) we obtain

$$\frac{4}{3}J_{1s} = \frac{(2+\beta_\ell^2)}{4}\left[|A_\perp^L|^2 + |A_\parallel^L|^2 + (L\to R)\right] + \frac{4m_\ell^2}{q^2}{\rm Re}\left(A_\perp^L A_\perp^{R*} + A_\parallel^L A_\parallel^{R*}\right) + 4\,\beta_\ell^2\left(|A_{0\perp}|^2 + |A_{0\parallel}|^2\right) + 4\,(4-3\beta_\ell^2)\left(|A_{t\perp}|^2 + |A_{t\parallel}|^2\right) + 8\sqrt{2}\frac{m_\ell}{\sqrt{q^2}}{\rm Re}\left[(A_\parallel^L + A_\parallel^R)A_{t\parallel}^* + (A_\perp^L + A_\perp^R)A_{t\perp}^*\right], \tag{B1}$$

$$\frac{4}{3}J_{1c} = |A_0^L|^2 + |A_0^R|^2 + \frac{4m_\ell^2}{q^2}\left[|A_t|^2 + 2\,{\rm Re}(A_0^L A_0^{R*})\right] + \beta_\ell^2|A_S|^2 + 8\,(2-\beta_\ell^2)|A_{t0}|^2 + 8\,\beta_\ell^2|A_{\parallel\perp}|^2 + 16\,\frac{m_\ell}{\sqrt{q^2}}{\rm Re}\Big[(A_0^L + A_0^R)A_{t0}^*\Big], \tag{B2}$$

$$\frac{4}{3}J_{2s} = \frac{\beta_\ell^2}{4}\left[|A_\perp^L|^2 + |A_\parallel^L|^2 + (L\to R) - 16\left(|A_{t\perp}|^2 + |A_{t\parallel}|^2 + |A_{0\perp}|^2 + |A_{0\parallel}|^2\right)\right], \tag{B3}$$

$$\frac{4}{3}J_{2c} = -\beta_\ell^2\left[|A_0^L|^2 + |A_0^R|^2 - 8\left(|A_{t0}|^2 + |A_{\parallel\perp}|^2\right)\right], \tag{B4}$$

$$\frac{4}{3}J_3 = \frac{\beta_\ell^2}{2}\Big[|A_\perp^L|^2 - |A_\parallel^L|^2 + (L\to R) + 16\left(|A_{t\parallel}|^2 - |A_{t\perp}|^2 + |A_{0\parallel}|^2 - |A_{0\perp}|^2\right)\Big], \tag{B5}$$

$$\frac{4}{3}J_4 = \frac{\beta_\ell^2}{\sqrt{2}}\mathrm{Re}\Big[A_0^L\,A_\parallel^{L\,*} + (L\to R) - 8\sqrt{2}\left(A_{t0}A_{t\parallel}^* + A_{\parallel\perp}A_{0\parallel}^*\right)\Big], \tag{B6}$$

$$\frac{4}{3}J_5 = \sqrt{2}\beta_\ell\,\mathrm{Re}\Big[A_0^L\,A_\perp^{L\,*} - (L\to R) - 2\sqrt{2}A_{t\parallel}A_S^* - \frac{m_\ell}{\sqrt{q^2}}\Big([A_\parallel^L + A_\parallel^R]A_S^* + 4\sqrt{2}\,A_{0\parallel}A_t^* - 4\sqrt{2}\,[A_0^L - A_0^R]A_{t\perp}^* - 4\,[A_\perp^L - A_\perp^R]A_{t0}^*\Big)\Big], \tag{B7}$$

$$\frac{4}{3}J_{6s} = 2\,\beta_\ell\,\mathrm{Re}\Big[A_\parallel^L\,A_\perp^{L\,*} - (L\to R) + 4\sqrt{2}\,\frac{m_\ell}{\sqrt{q^2}}\Big([A_\perp^L - A_\perp^R]A_{t\parallel}^* + [A_\parallel^L - A_\parallel^R]A_{t\perp}^*\Big)\Big], \tag{B8}$$

$$\frac{4}{3}J_{6c} = 4\,\beta_\ell\,\mathrm{Re}\Big[2\,A_{t0}A_S^* + \frac{m_\ell}{\sqrt{q^2}}\big[(A_0^L + A_0^R)A_S^* + 4\,A_{\parallel\perp}A_t^*\big]\Big], \tag{B9}$$

$$\frac{4}{3}J_7 = \sqrt{2}\beta_\ell\,\mathrm{Im}\Big[A_0^L\,A_\parallel^{L\,*} - (L\to R) + 2\sqrt{2}A_{t\perp}A_S^* + \frac{m_\ell}{\sqrt{q^2}}\Big([A_\perp^L + A_\perp^R]A_S^* + 4\sqrt{2}\,A_{0\perp}A_t^* + 4\sqrt{2}\,[A_0^L - A_0^R]A_{t\parallel}^* - 4\,[A_\parallel^L - A_\parallel^R]A_{t0}^*\Big)\Big], \tag{B10}$$

$$\frac{4}{3}J_8 = \frac{\beta_\ell^2}{\sqrt{2}}\,\mathrm{Im}\Big[A_0^L\,A_\perp^{L\,*} + (L\to R))\Big], \tag{B11}$$

$$\frac{4}{3}J_9 = \beta_\ell^2\,\mathrm{Im}\Big[A_\perp^L A_\parallel^{L\,*} + (L\to R))\Big], \tag{B12}$$

where the lepton mass m_ℓ has been kept and $\beta_\ell = \sqrt{1-4\,m_\ell^2/q^2}$.

Here the transversity amplitudes contain the contributions from the operators in Eqs. (3) – (5) which are factorizable. Non-factorizable contributions from $\mathcal{O}_{i\le 6,8}$ are taken into account by using effective Wilson coefficients $\mathcal{C}_i^{\rm eff}$. Within naive factorization the transversity amplitudes read

$$A_\perp^{L,R} = \sqrt{2}N\sqrt{\lambda}\Big\{\left[(\mathcal{C}_9 + \mathcal{C}_{9'}) \mp (\mathcal{C}_{10} + \mathcal{C}_{10'})\right]\frac{V}{M_B + M_{K^*}} + \frac{2m_b}{q^2}\,(\mathcal{C}_7 + \mathcal{C}_{7'})\,T_1\Big\}, \tag{B13}$$

$$A_\parallel^{L,R} = -N\sqrt{2}(M_B^2 - M_{K^*}^2)\times\Big\{\left[(\mathcal{C}_9 - \mathcal{C}_{9'}) \mp (\mathcal{C}_{10} - \mathcal{C}_{10'})\right]\frac{A_1}{M_B - M_{K^*}} + \frac{2m_b}{q^2}\,(\mathcal{C}_7 - \mathcal{C}_{7'})\,T_2\Big\}, \tag{B14}$$

$$A_0^{L,R} = -\frac{N}{2M_{K^*}\sqrt{q^2}}\times\Big\{\Big[(\mathcal{C}_9 - \mathcal{C}_{9'}) \mp (\mathcal{C}_{10} - \mathcal{C}_{10'})\Big]\Big[(M_B^2 - M_{K^*}^2 - q^2)(M_B + M_{K^*})A_1 - \frac{\lambda}{M_B + M_{K^*}}A_2\Big] + 2m_b\,(\mathcal{C}_7 - \mathcal{C}_{7'})\Big[\left(M_B^2 + 3M_{K^*}^2 - q^2\right)T_2 - \frac{\lambda}{M_B^2 - M_{K^*}^2}T_3\Big]\Big\}, \tag{B15}$$

$$A_t = N\frac{\sqrt{\lambda}}{\sqrt{q^2}}\left[2\,(\mathcal{C}_{10} - \mathcal{C}_{10'}) + \frac{q^2}{m_\ell}\frac{(\mathcal{C}_P - \mathcal{C}_{P'})}{(m_b + m_s)}\right]A_0, \tag{B16}$$

$$A_S = -2N\sqrt{\lambda}\,\frac{(\mathcal{C}_S - \mathcal{C}_{S'})}{(m_b + m_s)}A_0, \tag{B17}$$

$$A_{\parallel\perp\,(t0)} = \pm N\frac{\mathcal{C}_{T(5)}}{M_{K^*}}\left[(M_B^2 + 3\,M_{K^*}^2 - q^2)\,T_2\right. \tag{B18}$$

$$- \frac{\lambda}{M_B^2 - M_{K^*}^2} T_3 \Big],$$

$$A_{t\perp\,(0\perp)} = \pm 2N \frac{\sqrt{\lambda}}{\sqrt{q^2}} \mathcal{C}_{T(5)}\, T_1, \tag{B19}$$

$$A_{0\|\,(t\|)} = \pm 2N \frac{(M_B^2 - M_{K^*}^2)}{\sqrt{q^2}} \mathcal{C}_{T(5)}\, T_2. \tag{B20}$$

The upper and lower sign in Eqs. (B18)-(B20) refers C_T and C_{T5}, respectively. The normalization factor N is given as

$$N = G_F\, \alpha_e\, V_{tb} V_{ts}^* \sqrt{\frac{q^2\, \beta_\ell\, \sqrt{\lambda}}{3 \cdot 2^{10}\, \pi^5\, M_B^3}} \tag{B21}$$

and the $B \to K^*$ form factors V, $A_{0,1,2}$, $T_{1,2,3}$ are defined as in [4, 6, 8, 14, 21, 42].

The (SM+SM') calculation of the 4-fold differential decay rate by Krüger and Matias [6] already includes the chirality-flipped operators of the SM' basis for $m_\ell \neq 0$. We reproduce their results. The complete set of operators was considered in the limit $m_\ell = 0$ by Kim and Yoshikawa [20]. The extension to $m_\ell \neq 0$ for (S+P) operators has been performed by Altmannshofer *et al.* [8] within the transversity amplitude formalism. We agree with the arXiv v5 of this work [3].

The extension to $m_\ell \neq 0$ to include the tensor operators (T+T5) has been performed by Alok *et al.* [21, 43]. We agree with the arXiv v4 of reference [21][4] for all expressions except for the sign of the $A_{t\perp} A_S^*$ interference term in Eq. (B10).

Appendix C: $\bar{B} \to \bar{K}^*(\to \bar{K}\pi)\, \ell^+\ell^-$ Matrix Element

We present here the parametrization of the hadronic matrix element used to calculate the decay $\bar{B} \to \bar{K}^*(\to \bar{K}\pi)\, \ell^+\ell^-$,

$$\mathcal{M} = \mathcal{F}\Big(X_S \left[\bar{\ell}\ell\right] + X_P \left[\bar{\ell}\gamma_5\ell\right] + X_V^\mu \left[\bar{\ell}\gamma_\mu\ell\right] + X_A^\mu \left[\bar{\ell}\gamma_\mu\gamma_5\ell\right] + X_T^{\mu\nu} \left[\bar{\ell}\sigma_{\mu\nu}\ell\right] \Big). \tag{C1}$$

We define

$$\mathcal{F} = i \frac{G_F \alpha_e}{\sqrt{2}\pi}\, V_{tb} V_{ts}^*\, g_{K^*K\pi} D_V\, 2|\vec{p}_K|\,, \tag{C2}$$

[3] We thank the authors of [8] for confirming missing factors of 2 in Eqs. (3.31) and (3.32) in earlier versions and the journal version.

[4] We thank Murugeswaran Duraisamy for confirming numerous typos in the journal version and the arXiv versions prior to v4 of [21].

A	$0.812^{+0.013}_{-0.027}$	[46]	λ	0.22543 ± 0.00077	[46]
$\bar{\rho}$	0.144 ± 0.025	[46]	$\bar{\eta}$	$0.342^{+0.016}_{-0.015}$	[46]
$\alpha_s(M_Z)$	0.1176		τ_{B^+}	1.638 ps	[47]
$\alpha_e(m_b)$	1/133		τ_{B^0}	1.525 ps	[47]
$m_c(m_c)$	$(1.27^{+0.07}_{-0.09})$ GeV	[47]	M_{B^+}	5.2792 GeV	[47]
$m_b(m_b)$	$(4.19^{+0.18}_{-0.06})$ GeV	[47]	M_{B^0}	5.2795 GeV	[47]
$m_t^{\rm pole}$	(173.3 ± 1.1) GeV	[48]	M_{K^+}	0.494 GeV	[47]
m_e	0.511 MeV	[47]	M_{K^0}	0.498 GeV	[47]
m_μ	0.106 GeV	[47]	$M_{K^{*+}}$	0.89166 GeV	[47]
M_W	(80.399 ± 0.023) GeV	[47]	$M_{K^{*0}}$	0.89594 GeV	[47]
$\sin^2\theta_W$	0.23116 ± 0.00013	[47]			

TABLE III: The numerical input used in our analysis. We neglect the mass of the strange quark. τ_{B^0} (τ_{B^+}) denotes the lifetime of the neutral (charged) B meson. Here, λ denotes the CKM parameter in the Wolfenstein parametrization.

Observable	$\bar{B}^0 \to \bar{K}^0\ell^+\ell^-$	$B^- \to K^-\ell^+\ell^-$
$10^8 \times \langle BR\rangle_{4m_\mu^2..2.0}$	$6.44^{+2.07}_{-1.06}$	$6.92^{+2.22}_{-1.13}$
$10^8 \times \langle BR\rangle_{2.0..4.3}$	$7.50^{+2.56}_{-1.25}$	$8.08^{+2.75}_{-1.35}$
$10^7 \times \langle BR\rangle_{4.3..8.68}$	$1.38^{+0.51}_{-0.25}$	$1.48^{+0.55}_{-0.27}$
$10^7 \times \langle BR\rangle_{1.0..6.0}$	$1.63^{+0.56}_{-0.27}$	$1.75^{+0.60}_{-0.29}$
$10^8 \times \langle BR\rangle_{14.18..16.0}$	$3.40^{+1.79}_{-0.83}$	$3.65^{+1.92}_{-0.89}$
$10^8 \times \langle BR\rangle_{16.0..18.0}$	$3.09^{+1.76}_{-0.81}$	$3.31^{+1.89}_{-0.87}$
$10^8 \times \langle BR\rangle_{18.0..22.0}$	$3.18^{+2.01}_{-0.92}$	$3.41^{+2.16}_{-0.98}$
$10^8 \times \langle BR\rangle_{16.0..q^2_{\rm max}}$	$6.34^{+3.82}_{-1.75}$	$6.80^{+4.10}_{-1.88}$
$10^1 \times \langle F_H\rangle_{4m_\mu^2..2.0}$	$1.03^{+0.06}_{-0.12}$	$1.03^{+0.06}_{-0.12}$
$10^2 \times \langle F_H\rangle_{2.0..4.3}$	$2.37^{+0.18}_{-0.33}$	$2.37^{+0.18}_{-0.33}$
$10^2 \times \langle F_H\rangle_{4.3..8.68}$	$1.24^{+0.12}_{-0.20}$	$1.24^{+0.12}_{-0.20}$
$10^2 \times \langle F_H\rangle_{1.0..6.0}$	$2.54^{+0.20}_{-0.36}$	$2.55^{+0.20}_{-0.36}$
$10^3 \times \langle F_H\rangle_{14.18..16.0}$	$7.04^{+1.47}_{-1.96}$	$7.04^{+1.48}_{-1.97}$
$10^3 \times \langle F_H\rangle_{16.0..18.0}$	$6.93^{+1.66}_{-2.09}$	$6.93^{+1.66}_{-2.09}$
$10^3 \times \langle F_H\rangle_{18.0..22.0}$	$8.17^{+2.43}_{-2.84}$	$8.18^{+2.43}_{-2.84}$
$10^3 \times \langle F_H\rangle_{16.0..q^2_{\rm max}}$	$7.75^{+2.10}_{-2.54}$	$7.75^{+2.10}_{-2.55}$

TABLE IV: The SM predictions for $\bar{B}^0 \to \bar{K}^0\ell^+\ell^-$ and $B^- \to K^-\ell^+\ell^-$ decays in q^2 bins. For the large recoil region $q^2 \leq 8.68\,\text{GeV}^2$, we use the QCDF results [14, 19], and include all known power-suppressed contributions [15]. For the low recoil region $q^2 \geq 14.18\,\text{GeV}^2$ we use the OPE framework [28]. In both cases we employ $B \to K$ form factors, or extrapolations thereof, from Ref. [49].

and use $\vec{p}_K$, the three momentum of the $\bar{K}$ in the $\bar{K}\pi$ cms,

$$|\vec{p}_K| = \frac{\sqrt{\lambda\,(M_{K^*}^2, M_K^2, M_\pi^2)}}{2\, M_{K^*}}\,, \tag{C3}$$

and the kinematical function λ defined as usual

$$\lambda(a,b,c) = a^2 + b^2 + c^2 - 2(ab + ac + bc)\,. \tag{C4}$$

Using this parametrization, we obtain the hadronic ten-

Observable	$\bar{B}^0 \to \bar{K}^{*0}\ell^+\ell^-$	$B^- \to K^{*-}\ell^+\ell^-$
$10^7 \times \langle BR\rangle_{4m_\mu^2..2.0}$	$2.17^{+0.44}_{-0.40}$	$2.21^{+0.44}_{-0.40}$
$10^7 \times \langle BR\rangle_{2.0..4.3}$	$1.05^{+0.25}_{-0.23}$	$1.15^{+0.27}_{-0.25}$
$10^7 \times \langle BR\rangle_{4.3..8.68}$	$2.46^{+0.52}_{-0.49}$	$2.66^{+0.56}_{-0.53}$
$10^7 \times \langle BR\rangle_{1.0..6.0}$	$2.47^{+0.55}_{-0.51}$	$2.67^{+0.60}_{-0.56}$
$10^7 \times \langle BR\rangle_{14.18..16.0}$	$1.26^{+0.40}_{-0.34}$	$1.35^{+0.43}_{-0.37}$
$10^7 \times \langle BR\rangle_{16.0..q^2_{\rm max}}$	$1.47^{+0.45}_{-0.39}$	$1.57^{+0.48}_{-0.42}$
$10^1 \times \langle A_{\rm FB}\rangle_{4m_\mu^2..2.0}$	$1.08^{+0.22}_{-0.23}$	$1.08^{+0.22}_{-0.23}$
$10^2 \times \langle A_{\rm FB}\rangle_{2.0..4.3}$	$8.58^{+3.46}_{-3.00}$	$7.66^{+3.15}_{-2.75}$
$10^1 \times \langle A_{\rm FB}\rangle_{4.3..8.68}$	$-1.81^{+0.45}_{-0.46}$	$-1.81^{+0.44}_{-0.46}$
$10^2 \times \langle A_{\rm FB}\rangle_{1.0..6.0}$	$4.94^{+2.81}_{-2.52}$	$4.20^{+2.57}_{-2.33}$
$10^1 \times \langle A_{\rm FB}\rangle_{14.18..16.0}$	$-4.37^{+0.69}_{-0.71}$	$-4.37^{+0.69}_{-0.71}$
$10^1 \times \langle A_{\rm FB}\rangle_{16.0..q^2_{\rm max}}$	$-3.80^{+0.63}_{-0.67}$	$-3.80^{+0.63}_{-0.67}$
$10^1 \times \langle F_L\rangle_{4m_\mu^2..2.0}$	$3.17^{+0.75}_{-0.76}$	$3.43^{+0.78}_{-0.78}$
$10^1 \times \langle F_L\rangle_{2.0..4.3}$	$7.88^{+0.52}_{-0.61}$	$7.96^{+0.50}_{-0.59}$
$10^1 \times \langle F_L\rangle_{4.3..8.68}$	$6.61^{+0.69}_{-0.75}$	$6.63^{+0.68}_{-0.74}$
$10^1 \times \langle F_L\rangle_{1.0..6.0}$	$7.35^{+0.60}_{-0.70}$	$7.46^{+0.58}_{-0.67}$
$10^1 \times \langle F_L\rangle_{14.18..16.0}$	$3.63^{+0.51}_{-0.62}$	$3.63^{+0.51}_{-0.62}$
$10^1 \times \langle F_L\rangle_{16.0..q^2_{\rm max}}$	$3.38^{+0.26}_{-0.33}$	$3.38^{+0.26}_{-0.33}$
$10^1 \times \langle F_T\rangle_{4m_\mu^2..2.0}$	$6.83^{+0.76}_{-0.75}$	$6.58^{+0.78}_{-0.78}$
$10^1 \times \langle F_T\rangle_{2.0..4.3}$	$2.12^{+0.61}_{-0.52}$	$2.04^{+0.59}_{-0.50}$
$10^1 \times \langle F_T\rangle_{4.3..8.68}$	$3.39^{+0.75}_{-0.69}$	$3.37^{+0.74}_{-0.68}$
$10^1 \times \langle F_T\rangle_{1.0..6.0}$	$2.65^{+0.70}_{-0.60}$	$2.54^{+0.67}_{-0.58}$
$10^1 \times \langle F_T\rangle_{14.18..16.0}$	$6.37^{+0.62}_{-0.51}$	$6.37^{+0.62}_{-0.51}$
$10^1 \times \langle F_T\rangle_{16.0..q^2_{\rm max}}$	$6.62^{+0.33}_{-0.26}$	$6.62^{+0.33}_{-0.26}$
$10^1 \times \langle A_T^{(2)}\rangle_{14.18..16.0}$	$-3.68^{+1.96}_{-1.75}$	$-3.69^{+1.96}_{-1.75}$
$10^1 \times \langle A_T^{(2)}\rangle_{16.0..q^2_{\rm max}}$	$-6.03^{+1.50}_{-1.25}$	$-6.03^{+1.50}_{-1.25}$

TABLE V: The SM predictions for $\bar{B}^0 \to \bar{K}^{*0}\ell^+\ell^-$ and $B^- \to K^{*-}\ell^+\ell^-$ decays in q^2 bins. For the large recoil region $q^2 \le 8.68\,\text{GeV}^2$, we use the QCDF results [14], and include all known power-suppressed contributions [15]. For the low recoil region $q^2 \ge 14.18\,\text{GeV}^2$ we use the low recoil OPE framework [1, 4]. In both cases we use the $B \to K^*$ form factors, or extrapolations thereof, from [42]. Note that $\langle F_L\rangle + \langle F_T\rangle = 1$.

sors

$$X_S = -\frac{i}{4N}\cos\theta_K\, A_S\,, \tag{C5}$$

$$X_P = +\frac{i}{2N}\cos\theta_K\,\frac{m_\ell}{\sqrt{q^2}}\,A_t\,, \tag{C6}$$

$$\begin{aligned} X^\mu_{V,A} &= \frac{i}{4N}\cos\theta_K\,\varepsilon^\mu(0)\,(A_0^R \pm A_0^L) \\ &+ \frac{i}{8N}\sin\theta_K \\ &\times \Big(\varepsilon^\mu(+)\,e^{+i\phi}\Big[(A_\parallel^R + A_\perp^R) \pm (A_\parallel^L + A_\perp^L)\Big] \\ &+ \varepsilon^\mu(-)\,e^{-i\phi}\Big[(A_\parallel^R - A_\perp^R) \pm (A_\parallel^L - A_\perp^L)\Big]\Big), \end{aligned} \tag{C7}$$

$$\begin{aligned} X_T^{\mu\nu} &= \frac{\cos\theta_K}{N}\left(\varepsilon^\mu(t)\,\varepsilon^\nu(0)A_{t0} - \varepsilon^\mu(+)\,\varepsilon^\nu(-)A_{\parallel\perp}\right) \\ &+ \frac{\sin\theta_K}{\sqrt{2}N}\,\varepsilon^\mu(t) \\ &\times \left(\varepsilon^\nu(+)\,e^{i\phi}\,[A_{t\parallel} + A_{t\perp}] + \varepsilon^\nu(-)\,e^{-i\phi}\,[A_{t\parallel} - A_{t\perp}]\right) \\ &- \frac{\sin\theta_K}{\sqrt{2}N}\,\varepsilon^\mu(0) \\ &\times \left(\varepsilon^\nu(+)\,e^{i\phi}[A_{0\perp} + A_{0\parallel}] + \varepsilon^\nu(-)\,e^{-i\phi}[A_{0\perp} - A_{0\parallel}]\right), \end{aligned} \tag{C8}$$

where the polarization vectors $\varepsilon^\mu(n)$ in the $\bar{B}$ meson rest frame read [8]

$$\begin{aligned} \varepsilon^\mu(\pm) &= \frac{1}{\sqrt{2}}(0, 1, \mp i, 0)\,, \\ \varepsilon^\mu(0) &= \frac{1}{\sqrt{q^2}}(-q_z, 0, 0, -q_0)\,, \\ \varepsilon^\mu(t) &= \frac{1}{\sqrt{q^2}}(q_0, 0, 0, q_z)\,. \end{aligned} \tag{C9}$$

We choose the z-axis in this frame along the $\bar{K}^*$ direction of flight and q_0 (q_z) denotes the timelike (spacelike) component of the four momentum q^μ. The polarization vectors fulfill the completeness relations

$$\begin{aligned} g_{nn'} &= \varepsilon^\dagger_\mu(n)\,\varepsilon^\mu(n')\,, \\ g_{\mu\nu} &= \sum_{n,n'} \varepsilon^\dagger_\mu(n)\,\varepsilon_\nu(n')\,g_{nn'} \end{aligned} \tag{C10}$$

with $g_{nn'} = \text{diag}(+,-,-,-)$ for $n, n' = t, \pm, 0$. We use the relation Eq. (C10) to insert the full set of polarization vectors $\varepsilon^\mu(n)$ between the hadronic and leptonic currents, and introduce the helicity amplitudes $H_{an_1\ldots n_l}$ for arbitrary Dirac structures $\Gamma^{\mu_1\cdots\mu_l}$,

$$\langle \bar{K}^*(k,\eta(a))|\bar{s}\Gamma_{\mu_1\ldots\mu_l}b|\bar{B}(p)\rangle \tag{C11}$$

$$= \sum_{n_i,n_i'} \langle \bar{K}^*(k,\eta(a))|\bar{s}\Gamma^{\nu_1\ldots\nu_l}b|\bar{B}(p)\rangle \prod_{i=1}^{l} \varepsilon^\dagger_{\nu_i}(n_i) g^{n_i n_i'} \varepsilon_{\mu_i}(n_i')$$

$$\equiv \sum_{n_i} H^\Gamma_{an_1\ldots n_l} \prod_{i=1}^{l} g^{n_i n_i}\varepsilon_{\mu_i}(n_i)\,. \tag{C12}$$

The tensorial transversity amplitudes A_{ij} are related to the helicity amplitudes $H_{an_1n_2}$ by means of

$$\begin{aligned} A^\Gamma_{0\perp} &= \frac{1}{2}\big(H^\Gamma_{+0+} + H^\Gamma_{-0-}\big) & A^\Gamma_{0\parallel} &= \frac{1}{2}\big(H^\Gamma_{+0+} - H^\Gamma_{-0-}\big) \\ A^\Gamma_{t\perp} &= \frac{1}{2}\big(H^\Gamma_{+t+} - H^\Gamma_{-t-}\big) & A^\Gamma_{t\parallel} &= \frac{1}{2}\big(H^\Gamma_{+t+} + H^\Gamma_{-t-}\big) \\ A^\Gamma_{\parallel\perp} &= H^\Gamma_{0+-} & A^\Gamma_{t0} &= H^\Gamma_{0t0} \end{aligned} \tag{C13}$$

and

$$A_{ij} = 2\,N \sum_{\Gamma=T,T5} C_\Gamma A^\Gamma_{ij}\,. \tag{C14}$$

Note that the factor 2 above emerges from the relation $H^\Gamma_{aij} = -H^\Gamma_{aji}$, which is due to the asymmetry of $\sigma^{\mu\nu}$

under $\mu \leftrightarrow \nu$. The polarization vectors of the $\bar{K}^*$ for polarizations $a = \pm, 0$ in the $\bar{B}$ cms read

$$\begin{aligned} \eta^\mu(\pm) &= \frac{1}{\sqrt{2}}(0, 1, \pm i, 0)\,, \\ \eta^\mu(0) &= \frac{1}{M_{K^*}}(-q_z, 0, 0, M_B - q_0)\,. \end{aligned} \tag{C15}$$

This approach generalizes the concept of the transversity amplitudes, cf. e.g. Refs. [6, 8, 44], to which we also refer for the definition of the remaining transversity amplitudes A_i, $i = 0, \perp, \parallel, t, S$.
We employ $\gamma_5 = i/(4!)\,\varepsilon_{\alpha\beta\mu\nu}\gamma^\alpha\gamma^\beta\gamma^\mu\gamma^\nu$, such that

$$\begin{aligned} \mathrm{Tr}[\gamma^\alpha\gamma^\beta\gamma^\mu\gamma^\nu\gamma_5] &= 4\,i\,\varepsilon^{\alpha\beta\mu\nu}\,, \\ \sigma^{\alpha\beta}\gamma_5 &= -\frac{i}{2}\,\varepsilon^{\alpha\beta\mu\nu}\sigma_{\mu\nu} \end{aligned} \tag{C16}$$

with $\sigma_{\mu\nu} = i/2\,[\gamma_\mu, \gamma_\nu]$, and $\varepsilon_{0123} = -\varepsilon^{0123} = 1$.

Appendix D: $\bar{B} \to \bar{K}^{(*)}\ell^+\ell^-$ SM predictions

We update our SM predictions for $\bar{B} \to \bar{K}^*\ell^+\ell^-$ [4, 5] and $\bar{B} \to \bar{K}\ell^+\ell^-$ decays [28]. This includes the following improvements to the EOS [45] source code: Firstly, a common set of numerical input parameters is used, given in Table III. The resulting changes with respect to previous works are, however, marginal. Secondly, we improved the implementation of the subleading corrections within QCDF to the amplitudes in the region of large hadronic recoil. This concerns, in particular, the analytic expressions for the convolution integrals that involve the kaon light cone distribution amplitudes. The analytic results turn out to be more numerically stable than previous ones. In this process, we further switched from $\overline{\mathrm{MS}}$ to the charm pole mass. Lastly, we implemented all numerically relevant power-suppressed hard scattering and weak annihilation contributions [15]. Subleading $V_{ub}V_{us}^*$ contributions are included in the numerical analysis; Non-factorizable effects at low q^2 estimated in [49] are not included. The results are presented in Table IV and V. We recall that the q^2-region of validity within QCDF is approximately within $(1-7)\,\mathrm{GeV}^2$. Numerical predictions in the tables are extrapolations thereof and provided to match the experimental binning. Note that $\langle F_L\rangle + \langle F_T\rangle = 1$ [cf. Eq. (A8)], however, for convenience we give predictions for both observables. Since we calculated $\langle F_{L,T}\rangle$ individually the sum rule served as an independent check of the EOS code.
Besides the improvements mentioned above all details entering our low and large recoil predictions are given in [4, 5, 28]. Detailed SM predictions for $H_T^{(1,2,3)}$ are given in [4, 18].

[1] B. Grinstein and D. Pirjol, Phys. Rev. D **70**, 114005 (2004) [arXiv:hep-ph/0404250].
[2] M. Beylich, G. Buchalla and T. Feldmann, Eur. Phys. J. C **71**, 1635 (2011) [arXiv:1101.5118 [hep-ph]].
[3] B. Grinstein and D. Pirjol, Phys. Lett. B **533**, 8 (2002) [arXiv:hep-ph/0201298].
[4] C. Bobeth, G. Hiller and D. van Dyk, JHEP **1007**, 098 (2010) [arXiv:1006.5013 [hep-ph]].
[5] C. Bobeth, G. Hiller and D. van Dyk, JHEP **1107**, 067 (2011) [arXiv:1105.0376 [hep-ph]].
[6] F. Kruger and J. Matias, Phys. Rev. D **71**, 094009 (2005) [arXiv:hep-ph/0502060].
[7] C. Bobeth, G. Hiller and G. Piranishvili, JHEP **0807**, 106 (2008) [arXiv:0805.2525 [hep-ph]].
[8] W. Altmannshofer *et al.*, JHEP **0901**, 019 (2009) [arXiv:0811.1214 [hep-ph]].
[9] U. Egede, T. Hurth, J. Matias, M. Ramon and W. Reece, JHEP **0811**, 032 (2008) [arXiv:0807.2589 [hep-ph]].
[10] E. Lunghi and A. Soni, JHEP **1011**, 121 (2010) [arXiv:1007.4015 [hep-ph]].
[11] D. Becirevic and E. Schneider, Nucl. Phys. B **854**, 321 (2012) [arXiv:1106.3283 [hep-ph]].
[12] J. Matias, F. Mescia, M. Ramon and J. Virto, JHEP **1204**, 104 (2012) [arXiv:1202.4266 [hep-ph]].
[13] D. Das and R. Sinha, Phys. Rev. D **86**, 056006 (2012) [arXiv:1205.1438 [hep-ph]].
[14] M. Beneke, T. Feldmann and D. Seidel, Nucl. Phys. B **612**, 25 (2001) [arXiv:hep-ph/0106067].
[15] M. Beneke, T. Feldmann and D. Seidel, Eur. Phys. J. C **41**, 173 (2005) [arXiv:hep-ph/0412400].
[16] F. Kruger, L. M. Sehgal, N. Sinha and R. Sinha, Phys. Rev. D **61**, 114028 (2000) [Erratum-ibid. D **63**, 019901 (2001)] [arXiv:hep-ph/9907386].
[17] C. Hambrock and G. Hiller, Phys. Rev. Lett. **109**, 091802 (2012) [arXiv:1204.4444 [hep-ph]].
[18] F. Beaujean, C. Bobeth, D. van Dyk and C. Wacker, JHEP **1208**, 030 (2012) [arXiv:1205.1838 [hep-ph]].
[19] C. Bobeth, G. Hiller and G. Piranishvili, JHEP **0712**, 040 (2007) [arXiv:0709.4174 [hep-ph]].
[20] C. S. Kim and T. Yoshikawa, arXiv:0711.3880 [hep-ph].
[21] A. K. Alok, A. Datta, A. Dighe, M. Duraisamy, D. Ghosh and D. London, JHEP **1111**, 121 (2011) [arXiv:1008.2367 [hep-ph]].
[22] K. G. Chetyrkin, M. Misiak and M. Munz, Phys. Lett. B **400**, 206 (1997) [Erratum-ibid. B **425**, 414 (1998)] [hep-ph/9612313].
[23] A. Ali, G. Kramer and G. h. Zhu, Eur. Phys. J. C **47**, 625 (2006) [arXiv:hep-ph/0601034].
[24] K. S. M. Lee, Z. Ligeti, I. W. Stewart and F. J. Tackmann, Phys. Rev. D **75**, 034016 (2007) [arXiv:hep-ph/0612156].
[25] C. Bobeth, P. Gambino, M. Gorbahn and U. Haisch, JHEP **0404**, 071 (2004) [hep-ph/0312090].
[26] T. Huber, E. Lunghi, M. Misiak and D. Wyler, Nucl. Phys. B **740**, 105 (2006) [hep-ph/0512066].
[27] A. Bharucha, T. Feldmann and M. Wick, JHEP **1009**, 090 (2010) [arXiv:1004.3249 [hep-ph]].
[28] C. Bobeth, G. Hiller, D. van Dyk and C. Wacker, JHEP **1201**, 107 (2012) [arXiv:1111.2558 [hep-ph]].
[29] T. Aaltonen *et al.* [CDF Collaboration], Phys. Rev. Lett.

108, 081807 (2012) [arXiv:1108.0695 [hep-ex]].
[30] R. Aaij *et al.* [LHCb Collaboration], arXiv:1209.4284 [hep-ex].
[31] J. -T. Wei *et al.* [BELLE Collaboration], Phys. Rev. Lett. **103**, 171801 (2009) [arXiv:0904.0770 [hep-ex]].
[32] J. P. Lees *et al.* [BABAR Collaboration], Phys. Rev. D **86**, 032012 (2012) [arXiv:1204.3933 [hep-ex]].
[33] H. Miyaki, "CDF results on the search for rare $B_{d,s} \to \mu^+\mu^-$ and $X_s\mu^+\mu^-$ decays". Talk presented at "ICHEP 2012", July 4-11, 2012, Melbourne, Australia. http://www-cdf.fnal.gov/physics/new/bottom/120628.blessed-b2smumu_96/
[34] [ATLAS Collaboration], [CMS Collaboration], [LHCb Collaboration], ATLAS-CONF-2012-061, CMS-PAS-BPH-12-009, LHCb-CONF-2012-017, http://cdsweb.cern.ch/record/1452186/files/LHCb-CONF-2012-017.pdf
[35] K. De Bruyn *et al.* Phys. Rev. Lett. **109**, 041801 (2012) [arXiv:1204.1737 [hep-ph]].
[36] F. Borzumati, C. Greub, T. Hurth and D. Wyler, Phys. Rev. D **62**, 075005 (2000) [hep-ph/9911245].
[37] C. Bobeth and U. Haisch, arXiv:1109.1826 [hep-ph].
[38] D. Becirevic and A. Tayduganov, arXiv:1207.4004 [hep-ph].
[39] J. Matias, Phys. Rev. D **86**, 094024 (2012) [arXiv:1209.1525 [hep-ph]].
[40] T. Blake, U. Egede and A. Shires, arXiv:1210.5279 [hep-ph].
[41] R. Aaij *et al.* [LHCb Collaboration], Phys. Rev. Lett. **108**, 181806 (2012) [arXiv:1112.3515 [hep-ex]].
[42] P. Ball and R. Zwicky, Phys. Rev. D **71**, 014029 (2005) [hep-ph/0412079].
[43] A. K. Alok, A. Dighe, D. Ghosh, D. London, J. Matias, M. Nagashima and A. Szynkman, JHEP **1002**, 053 (2010) [arXiv:0912.1382 [hep-ph]].
[44] A. Faessler, T. Gutsche, M. A. Ivanov, J. G. Korner and V. E. Lyubovitskij, Eur. Phys. J. direct C **4**, 18 (2002) [arXiv:hep-ph/0205287].
[45] D. van Dyk *et al.* [EOS Collaboration], EOS: A HEP Program for Flavor Observables, http://project.het.physik.tu-dortmund.de/eos/
[46] J. Charles *et al.* [CKMfitter Group Collaboration], Eur. Phys. J. **C41**, 1-131 (2005). [hep-ph/0406184]. We use the numerical results as presented at ICHEP10.
[47] K. Nakamura *et al.* [Particle Data Group], J. Phys. G **37**, 075021 (2010).
[48] [Tevatron Electroweak Working Group and CDF Collaboration and D0 Collab], arXiv:0903.2503 [hep-ex].
[49] A. Khodjamirian, T. Mannel, A. A. Pivovarov and Y. M. Wang, JHEP **1009**, 089 (2010) [arXiv:1006.4945 [hep-ph]].